OPTIMAL OPERATION OF MICROGRID UNDER A STOCHASTIC ENVIRONMENT

by

ZHAOHAO DING

Presented to the Faculty of the Graduate School of
The University of Texas at Arlington in Partial Fulfillment
of the Requirements
for the Degree of

DOCTOR OF PHILOSOPHY

THE UNIVERSITY OF TEXAS AT ARLINGTON
May 2015

Acknowledgements

I would like to express deepest gratitude to my supervising professor, Dr. Wei-Jen Lee for his guidance and support throughout my entire doctoral program. His unlimited patience and encouragement are above and beyond appreciation. He is not only my academic advisor but also a life-time mentor.

My sincere thanks are extended to Dr. Ali Davoudi, Dr. William E. Dillon, Dr. Rasool Kenarangui and Dr. David A. Wetz for their valuable instructions and serving as my dissertation committee members. Meanwhile, I wish to thank all the members of Energy Systems Research Center at the University of Texas at Arlington for their friendship in the last five years. It is them who make my stressful graduate life much more fun.

Last but not the least, I would delicate my dissertation to my parents and my dear, Lin Zhou. Although they are on the other side of the Pacific Ocean, they have been my constant source of encouragement and support. Without their enduring trust and love, this work will by no means be accomplished.

March 25, 2015

Abstract

OPTIMAL OPERATION OF MICROGRID UNDER

A STOCHASTIC ENVIRONMENT

Zhaohao Ding, PhD

The University of Texas at Arlington, 2015

Supervising Professor: Wei-Jen Lee

With its technological and regulatory innovation of scale and structure, microgrids have been developed all over the world as a mean to address the high penetration level of renewable generation, reduce the greenhouse gas emission, and provide economical solutions for the currently non-electrified area. The operation of microgrid requires resource planning for those fossil-fuel based generators, energy storage systems, and demand resources if demand side management is implemented. Due to the stochastic nature of renewable energy resources, load behaviors and market prices, enormous uncertainties are involved in the microgrid operation and scheduling problems for both short-term and longer term. These uncertainties may result in a non-optimal operation or even jeopardizing the reliability of the microgrid if they are not fully considered in the scheduling stage.

This dissertation applies stochastic modeling and optimization techniques to address the challenges brought by uncertainties in the microgrid operation through. The microgrid day-ahead scheduling problem, demand side management scheduling problem, and medium-term operation scheduling problem are modelled via stochastic approaches to achieve the optimal operation decisions under an environment with high

degree of uncertainties. Meanwhile, a microgrid carbon emission co-optimized scheduling algorithm is also proposed to address the carbon emission in the microgrid operation. Correspondingly, the uncertainty models and solving methods for those formulations are also proposed by this dissertation and numerical results are presented for verification and illustration purpose.

Table of Contents

List of Illustrations

List of Tables

Chapter 1

Introduction

1.1 Definition of Microgrid

Demand for electricity is rapidly increasing thereby applying pressure to expand generation and distribution capacity worldwide. The expansion of traditional services not only imposes burdens on financial resources but also encounters many challenges from community who oppose the construction of new power generation plants or transmission facilities in their backyard. From the integrated resource planning point of view, a feasible and economical remedy is, therefore, to utilize existing dispersed generation capacity known as distributed generation (DG) and/or renewable energy resources that may exist in the vicinity of the load centers.

DGs have existed in the market for many years. The main criteria for selecting the type of fuel source for a DG is its local availability, conversion system technological advancement, impact on the environment, and operating cost. Large diesel or gas powered generation sets are used in stand-by mode to power up vital services such as hospitals, financial and commercial compounds, telecommunication centers, and industrial premises. Wind turbines, photovoltaic (PV) energy sources, and fuel cells are new comers that are now competing in size, per kW cost, and efficiency with many standard generating sets. Today's DGs cost rate ($/kWhr) is becoming more and more competitive as efficiency/technology behind the modern energy conversion units is continuously being improved and diversified. By combining a variety of dispersed DGs, a distributed energy resource (DER) domain is developed. Various mixtures of different energy sources are then controlled under a central energy management system (EMS) in order to improve efficiency and reliability of the operation. As incorporated the modern concept of DER and EMS theory, the microgrid concept is put forwarded [1].

As newly created concept, there are various definitions existing for the microgrid. In 2002, Consortium for Electric Reliability Technology Solutions (CERTS), as one of the earliest organization conducting microgrid research, brought up the microgrid definition [2] as following.

> The Consortium for Electric Reliability Technology Solutions (CERTS) microgrid concept assumes an aggregation of loads and microsources operating as a single system providing both power and heat. The majority of the microsources must be power electronic based to provide the required flexibility to insure operation as a single aggregated system. This control flexibility allows the CERTS MicroGrid to present itself to the bulk power system as a single controlled unit that meets local needs for reliability and security.

Department of Energy (DOE), which is another pioneer that conducts microgrid and DG research, also provided their perspective on the concept of microgrid. In a workshop held by DOE in 2012, DOE adopted the following statement as the definition of microgrid [3].

> A microgrid is a group of interconnected loads and distributed energy resources within clearly defined electrical boundaries that acts as a single controllable entity with respect to the grid. A microgrid can connect and disconnect from the grid to enable it to operate in both grid-connected or island-mode.

As another important entity which leads lots of microgrid research, Department of Defense (DOD) also provided their specific definition of microgrid [4] as shown below.

> A DoD installation microgrid is an integrated energy system consisting of interconnected loads and energy resources which, as an integrated system, can island from the local utility grid and function as a stand-alone system.

It can be observed from those three definitions that although different entities have various perspectives on microgrid, the common concept can be extracted that microgrid is a bunch of electrical loads within certain geographic boundary powered by local distributed energy resources (DER) which include DGs and energy storage system (ESS). In such a system, wind turbines, PV panels and other renewable generations can

be used as DGs and the stability and reliability should be maintained by the system itself with the help of modern operation and control techniques. Furthermore, such a system can be either connected to the utility grid or operated in an islanded mode. In this dissertation, both operation modes are investigated and the corresponding decision-making model is proposed respectively.

1.2 Microgrid Facility Examples

As an alternative approach to power up dispersed loads and to utilize renewable energy resources, microgrid has been investigated intensively and numbers of microgrid facilities have been designed and implemented all over the world. Research organizations and commercial entities are kept focusing on the development and implementation of microgrid to improve and strengthen the current power infrastructure. The experiment setting and operation objectives are various on a large span [5].

1.2.1 European Union (EU)

EU pays lots of attention to the level of climate change thus there are certain targets has been set for the member states to achieve by 2020. The European Parliament has passed several directives such as 2001/77/EC, 2003/30/EC and 2006/32/EC. Those documents gave certain reduction requirements for carbon emissions. Consequently, the renewable energy resources penetration level should be increased to compensate the reduced traditional fossil generation. Meanwhile, higher energy efficiency is also motivated by those directives. Since microgrid has been considered as a prospective approach to utilize renewable energy, there are several microgrid projects conducting in EU member states.

From the EU international level, there are two major microgrid research projects. The first project funded by EU was the ‘Microgrids: Large Scale Integration of Micro-Generation to Low Voltage Grids’ which was undertaken by a consortium led by National

Technical University of Athens (NTUA), included 14 partners from seven EU countries, including utilities such as EdF (France), PPC (Greece), and EdP (Portugal); manufacturers, such as SMA, GERMANOS, and URENCO; plus research institutions and universities such as Labein, the University of Manchester, and ISET Kassel. With €4.5 million grant, this project was designed to investigate the dynamics of DGs in a microgrid and developing different control, operation and protection schemes. A test microgrid was installed on the Kythnos Island, Greece [6], as shown in Figure 1-1. Another microgrid study facility, as shown in Figure 1-2, was installed in ISET, Germany [5] to conduct control strategy researches. A microgrid prototype with Flywheel energy storage was installed in University of Manchester, for exploring the energy storage technologies.

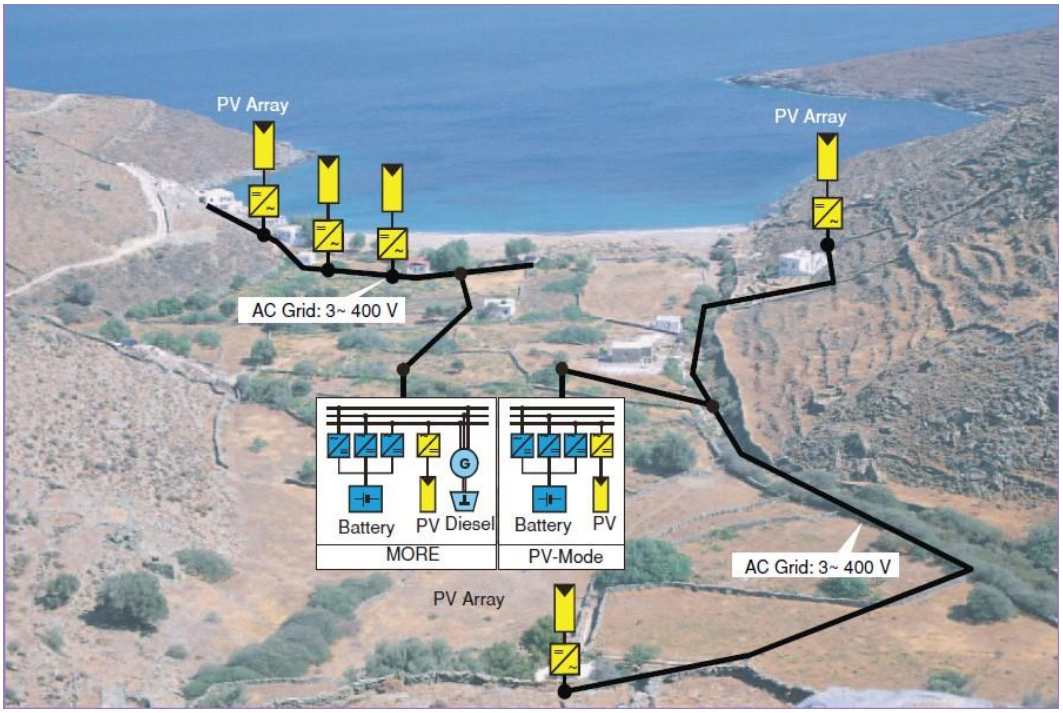

Figure 1-1 Test microgrid in Kythonos Island

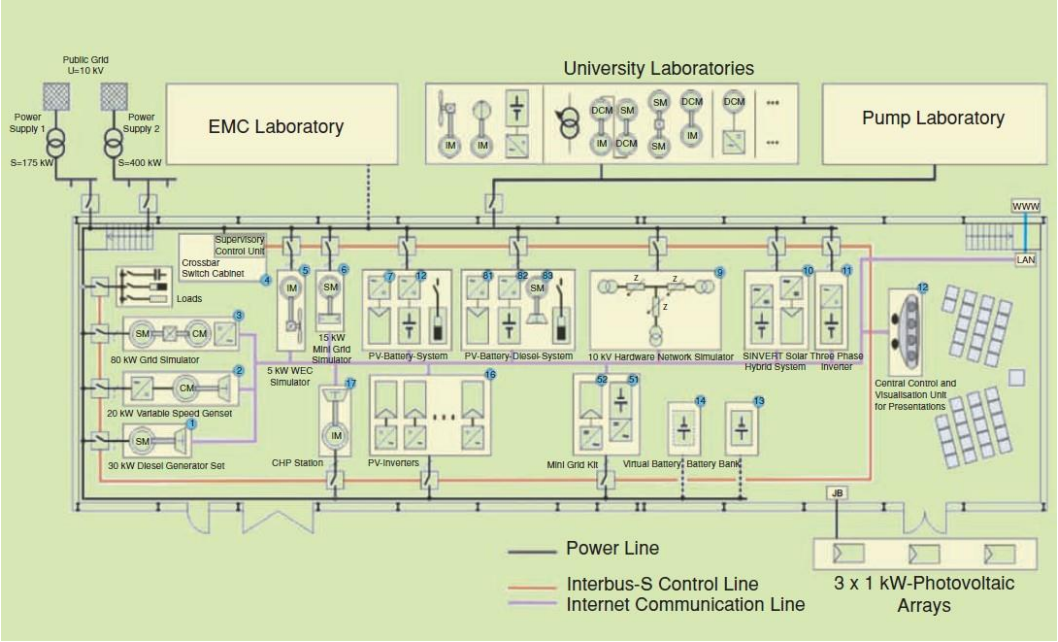

Figure 1-2 Microgrid laboratory facilities at ISET

As a follow-up, a project named ‘More Microgrids: Advanced Architectures and Control Concepts for More Microgrids’ was funded at €8.5 million. This project, again, was undertaken by a consortium led by NTUA. This project was intent to investigate alternative control and protection strategies along with plug-and-play concepts. A residential demonstration, which involved 1200-inhabitant ecological estate in Mannheim-Wallstadt, has been prepared as a continuous long-term field test for this project [7].

1.2.2 Japan

Japan is one of current world leaders in microgrid demonstration projects. Motivated by its limited natural resources, Japanese Government set ambitious target for utilizing more renewable energy resources. However, the intermittence characteristics of renewable energy might have a negative effect on Japan’s world-wide recognized power quality reputation. Microgrid is treated as a potential solution for this problem by Japan Government. Therefore, several microgrid projects are implemented in Japan.

Traditionally, the intermittent renewable energy sources make the residual purchases from utility varies a lot. In a microgrid with energy storage devices, the intermittent renewable supply can be compensate by itself so from the grid point of view, the microgrid become a constant/dispatchable load. Japan emphasized this principle a lot in its implementations.

The New Energy and Industrial Technology Development Organization (NEDO) started to sponsor three microgrid demonstrations under its 'Regional Power Grid with Renewable Energy Resources Project' in 2003 [8].

The first project started to operate in October 2005 World Exposition in Aichi and was moved to Tokoname City in 2006. Its main feature is using fuel cells as the main sources. There are two (270kW and 300kW) molten carbonate fuel cells (MCFCs), four 200kW phosphoric acid fuel cells (PAFCs), and a 50kW solid oxide fuel cell (SOFC).

The second demonstration is the Aomori project in Hachinohe, which is undertaken by the Mitsubishi Research Institute and Mitsubishi Electric. This system has its private distribution line and consists of PV systems, wind turbines, gas engines and storage. The energy management system (EMS) developed through this project optimally meets combined heat and electric demand.

The third project is installed in Kyotango, which has a biogas plant connected to two PV systems and a small wind turbine. This network operates with communication links by internet protocol to balance the supply and load.

Also, there are some private microgrid projects. For example, Shimizu Corporation, cooperated with University of Tokyo, developed a microgrid testbed in Tokyo. Also, Tokyo Gas created an integrated DG control through simulations and experiments in Yokohama [8].

1.2.3 United States

The United States, as the world-leading energy research country, has expanding microgrids research projects. Among all those microgrid research facilities, the most well-known project is CERTS microgrid. It is a collaboration project undertaken by AEP, TECOGEN, Northern Power Systems, S&C Electric Co, Sandia National Laboratories, and the University of Wisconsin. It consists of several DGs and a thyristor based switch to allow isolation from the grid [2, 5, 9]. The CERTS microgrid is intended to achieve a seamless back up to continue the service from utility service interruption. CERTS microgrid tried to provide this kind of service for relatively small size (less 2MW peak load). Also CERTS tried to make the system as robust as possible which means there is no single device is essential for operation. The schematic example of CERTS microgrid is shown in Figure 1-3 [6].

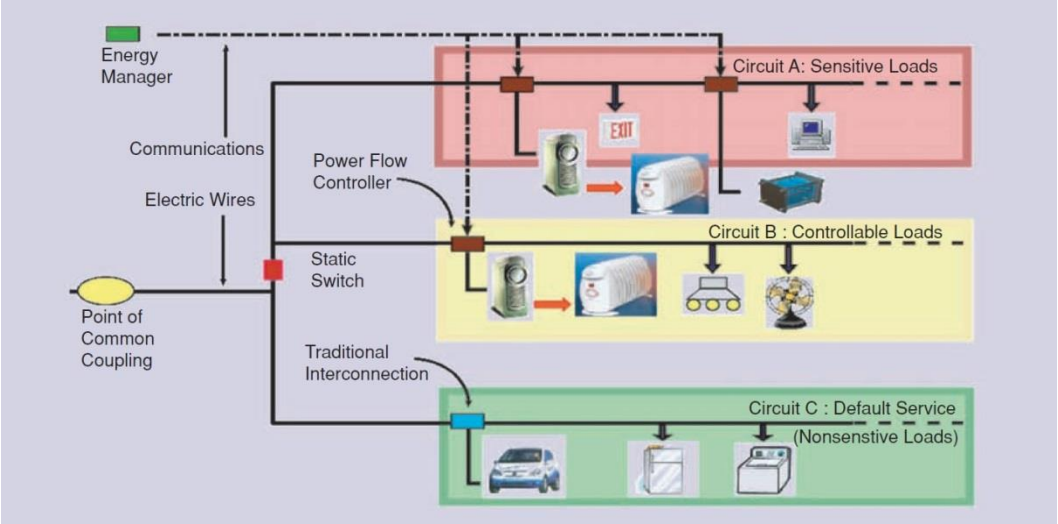

Figure 1-3 Schematic of an example CERTS microgrid

Besides CERTS project, there are some other research activities regarding microgrid. DOE also grants US$4 million to General Electric (GE) Global Research for microgrid research [5]. This project is aimed to develop and demonstrate a microgrid

energy management framework for various applications that provides a control, protection and operation platform. The energy management framework is designed to provide intelligent control for both generation and load considering the low inertia of those power electronics devices.

Also, there are some campus microgrid facilities in US. Among those the largest one is installed at Illinois Institute of Technology (IIT) called ‘perfect power system’ [10]. This US$14 million project is undertaken by IIT cooperated with S&C Electric, Endurant Energy, and ComEd. A microgrid system is designed for IIT’s main campus. The objective of this project is to provide a flagship system for other universities, municipalities as a solution the nation’s energy crisis. The system schematic is shown in Figure 1-4 [10].

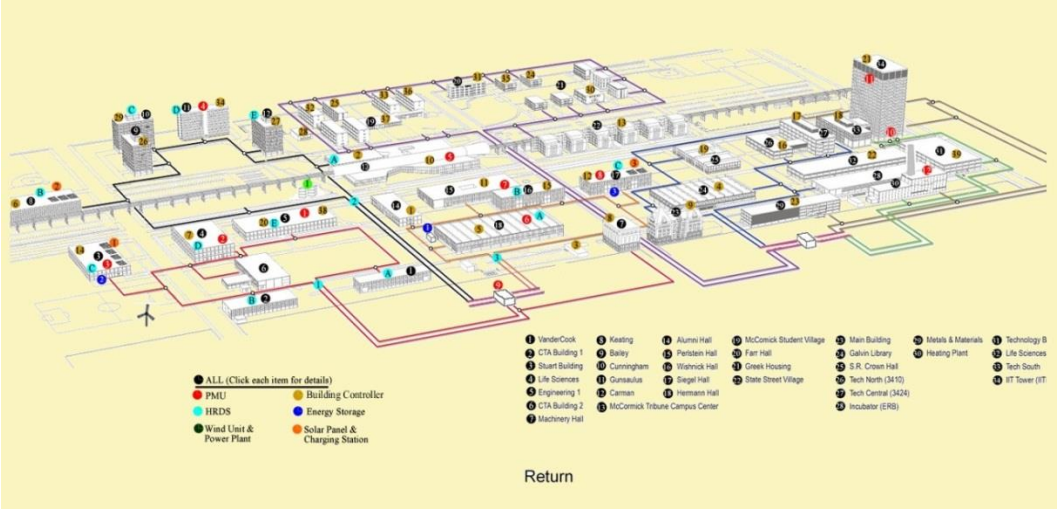

Figure 1-4 System schematic of microgrid in IIT campus

In the University of Texas at Arlington (UTA) campus, another microgrid testbed is designed and installed with the DOE grant [5]. This project contains three sub-microgrid which all equipped with hierarchical control systems. The control and communication are realized based on CompactRIO controllers from National Instruments

[11]. The optimal operation strategies and other research topics are investigated based on this microgrid testbed. The schematic of this microgrid is shown in Figure 1-5 and the layout of indoor part of this smart microgrid testbed is shown in Figure 1-6.

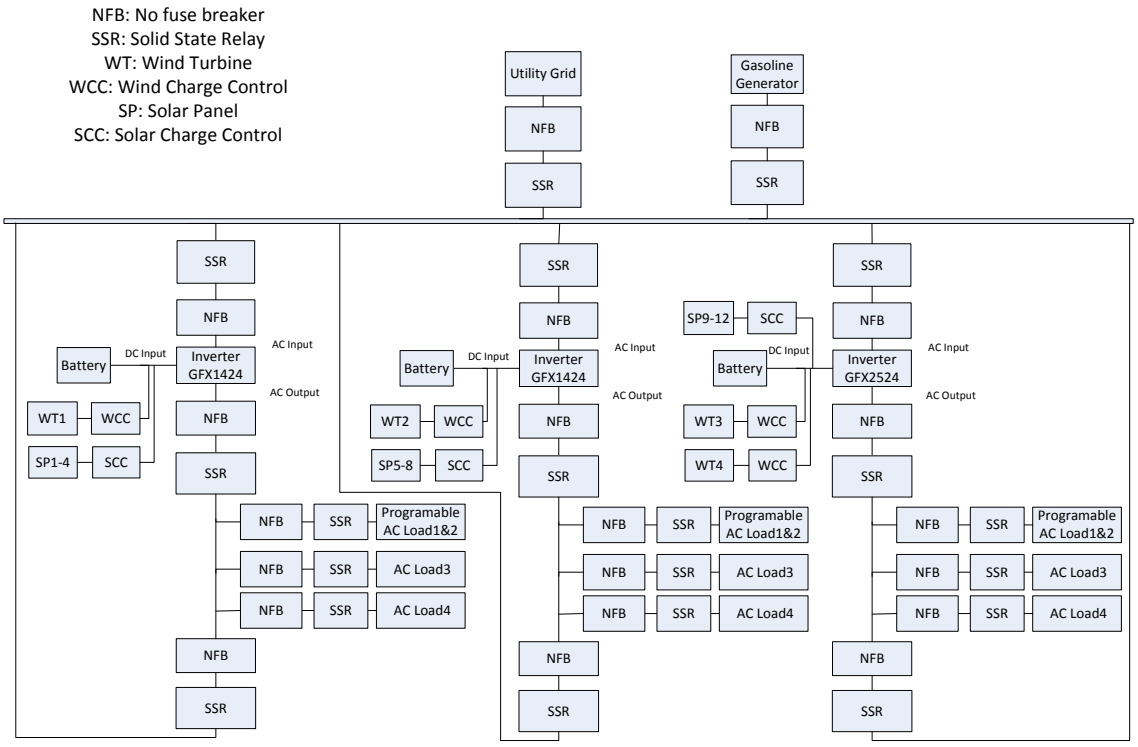

Figure 1-5 Architecture of the microgrid testbed in UTA campus

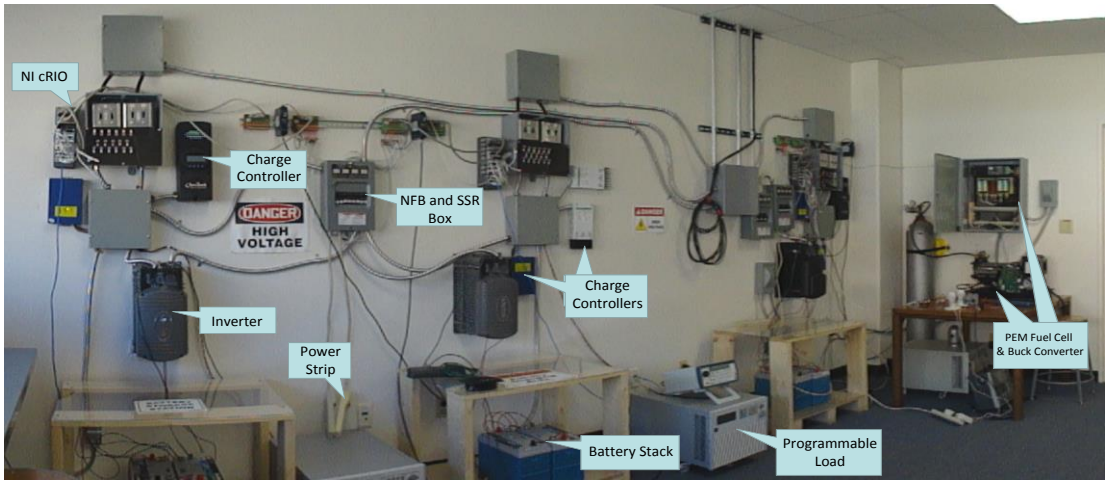

Figure 1-6 Indoor layout of microgrid testbed in UTA campus

1.3 Benefits of Implementing Microgrid

It can be summed up from the designing principle and all those on-going and demonstration projects that microgrid bring lots exciting benefits and opportunities. Those merits of implementing microgrid are summarized as the following.

First of all, implementing microgrid has the potential to reduce the dependency on imported fuel sources and help in regulating prime fuel market competition. The increase interest in DERs, which including multiple types of energy sources, can influence the market and level of competition for prime sources of energy. Developing countries such as China and India have started to build a rapidly moving production infrastructure that needs more energy. This has resulted, among other factors, in pushing the global prime fuel market to a record high. With the public support and encouragement following the dynamically changing of fuel prices and environmental concern over global warming, current DG's technologies can compete with the traditional generation facilities. Profitable DG's are fueled by available local prime fuel sources rather than imported ones. The DG market thrust is obviously driven by the economic benefits to be gained by all involved parties along with the positive environmental impact of using local resources.

Secondly, implementing microgrid can improve the utilization of renewable generation resources. Although renewable energy conversion systems are characterized by their intermittent energy nature, they have minimal environmental impact and offer free replenishment of the prime fuel source. Many countries have an abundance of natural and renewable resources that can be effectively integrated to meet a portion of the demand. Due to its innovative architecture and intelligent interface, microgrid can be a good entity to integrate high penetration level of renewable energy. Also, the grid-connected microgrid, which cooperated with ESS and responsive load, can make the power flow on the point of common coupling (PCC) smoother thus reduce the generation fluctuation caused by intermittence nature of renewable generation from the utility point of view.

Moreover, implementing microgrid can enhance the demand side management (DSM). Considering the deployment of advanced meter infrastructure (AMI) and delicate communication system, microgrid is capable of optimally managing its demand side without requiring further investment. The AMI system installed in the microgrid can be a useful tool for load pattern recognition and demand forecasting [12]. Also, the relatively small scale makes microgrid system operators easier to categorize different load groups based on their load characteristics and price responsiveness. In such a manner, the managing of demand side for microgrid can be further improved.

Furthermore, implementing microgrid can defer the construction or extension of transmission lines. Microgrid can be used to support demand during peak periods, thus eliminating the need for installing peak generation units and enhance security benefits [13]. Also, microgrid can be used to meet the heat and electricity demand for nearby industrial and commercial areas, thus relieving the centralized power plant from

dispatching power over long distances for heating purposes and improving the fuel/kWhr ratio.

Last but not the least, implementing microgrid can help rural electrification, especially for the under-developed areas. Currently, many developing and third world countries are in need of a rural electrification resolution. Over 1.2 billion people are without accessing to electricity. About 2.8 billion people still use solid fuels for cooking and heating. African and southeastern countries in particular have the largest percentage of rural darkness [14]. Such countries do not have the capacity or resources to build large centralized generation plants or transmission infrastructure although the sector and its services are an important driver for the country's economic development and welfare [15]. The opportunity for microgrid in various scales is evident when one considers with the availability of local renewable energy resources such as solar and wind. As incorporated with modern EMS system, dispersed microgrids can be a solution with less financial burden to meet the demand of those rural communities [16].

1.4 Challenges for Microgrid Operation

As mentioned in the previous sections, there are numbers of benefits of implementing microgrid. However, it is necessary for the microgrid to maintain a stable and reliable operation to achieve those benefits. Due to its unique characteristics, there are multiple challenges for the microgrid operation.

Considering the penetration level of renewable generation, the volatility of renewable energy resources can impact the operation of microgrid significantly, as shown in Figure 1-7 [17]. Those types of volatilities pose uncertainties in the microgrid operation, especially in the microgrid resource scheduling. Currently, most of the large power system operators try to use renewable generation forecasting to alleviate the uncertainties in their scheduling. However, because of the stochastic nature of renewable

energy resource, it is almost impossible to achieve a no-mismatch forecasting results with current techniques. For example, as shown in Figure 1-8 [18], for the hour ending at 19:00, the day-ahead forecasting predicted about 1300 MW from the wind generation while the actual output was 400 MW during the operation hour. The shortage of 900MW may lead to severe reliability problems. Due to the geographic scale of microgrid, the prediction for the renewable generation in a microgrid are particularly difficult thus the forecasting errors are more significant than those for bulk power system. This kind of uncertainties brings considerable challenges for the resource scheduling of microgrid operation.

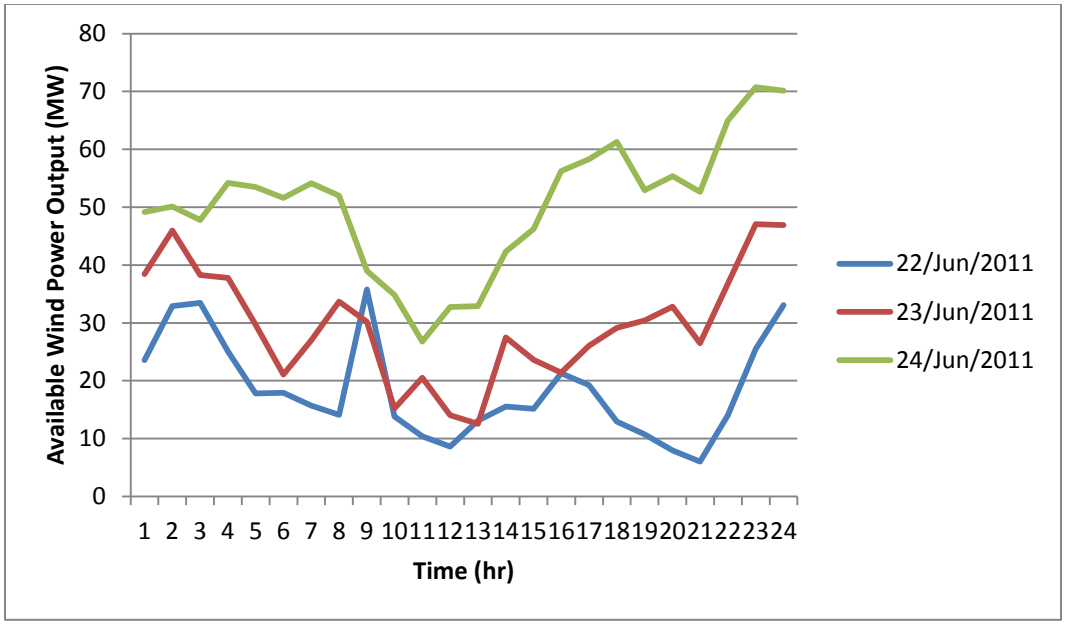

Figure 1-7 Three consecutive day wind power output for a wind farm in Oklahoma

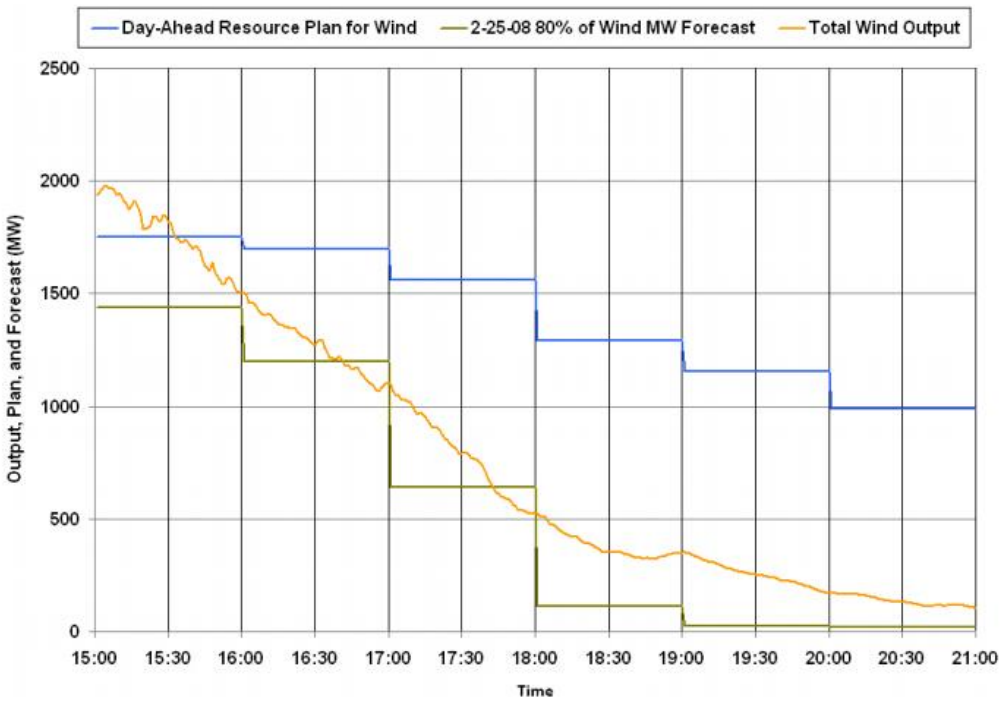

Figure 1-8 Wind forecasting mismatch in ERCOT on 02/26/2008

Another challenge faced by microgrid operation is the mismatch between renewable generation and load pattern. This phenomenon is observed more in wind power production. For example, as shown in Figure 1-9 [19], during the load peak the wind power production is low. However, the wind generation is high during the off-peak hours. In microgrid, similar type of mismatch occurs due to the same reason since the penetration level of renewable generation in microgrid might be even higher than bulk power system. This type of mismatch can lead to operational challenges when microgrid trying to integrate large amount of wind energy. Consequently, the utilization factor of renewable energy resources would be jeopardized. Also, this type of mismatch also shows uncertain behaviors. It can be difficult to fully capture the mismatch in the day-ahead forecasting results [20].

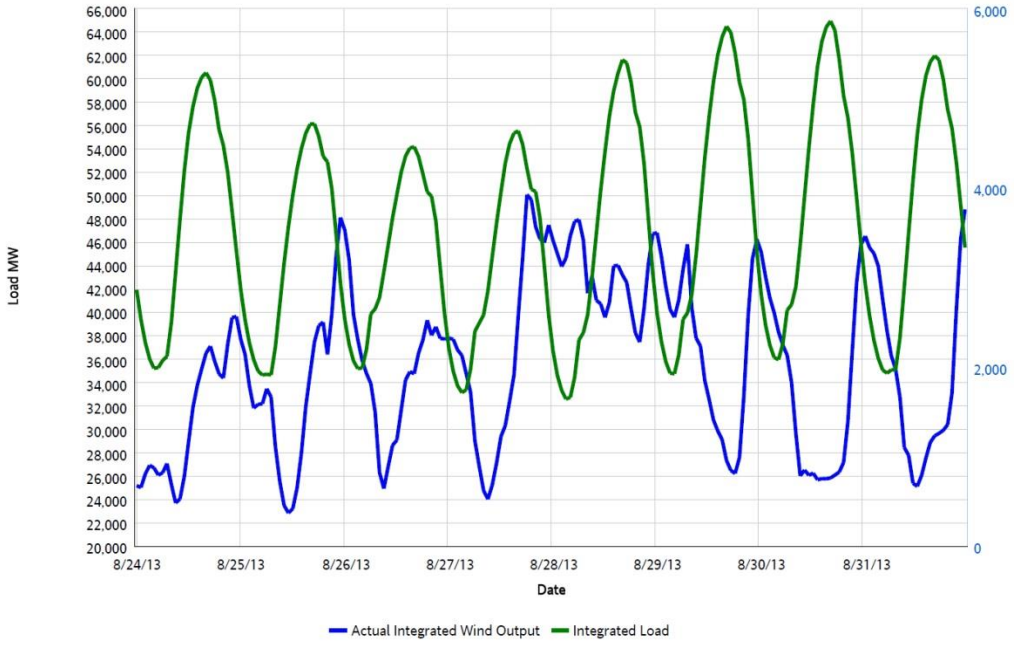

Figure 1-9 ERCOT load and wind power production in August, 2013

Moreover, microgrid operation is challenged to optimally participate in the deregulated market under the current market framework. For a grid-connected microgrid, it is assumed as a 'modern citizen' from the bulk power system point of view [5]. Consequently, there are numbers of opportunities for microgrid to participate in the power market. For example, in current ERCOT market the offer price cap keeps increasing since the nodal market opened in 2010 [21], as shown inTable 1-1. Those scarcity price scenarios create financial opportunities for microgrid. The optimal operation scheme should be developed to help the stakeholders of microgrid harvest the maximum economic benefit by strategically participating in the power market.

Table 1-1 Offer Price Cap in ERCOT since 2010

Start Time	12/2010	09/2012	06/2013	06/2014	06/2015
Price Cap in ERCOT Market ($/MWh)	3000	4500	5000	7000	9000

1.5 Summary

To sum up, microgrid is a promising electric infrastructure that has numbers of benefits from both economic and environmental perspectives. However, to achieve those exciting advantages of microgrid, there are several obstacles and challenges in the microgrid operation, such as uncertainties in the resource scheduling, mismatch in renewable power production and load curve, and deregulated market participation. In this study, operation schemes are proposed to address those challenges respectively. For those problems with uncertainties involved, the randomness is modeled by Monte Carlo simulation and solved by stochastic optimization method. For the mismatch of renewable generation and daily load curve, an internal pricing based demand side management scheme is proposed when considering the uncertainties parameters in the formulation. For the participation in the deregulated market, an optimal operation framework is also proposed.

The rest of the dissertation is organized as follows. Chapter 2 presents the uncertainty models and mathematical methods that are used for stochastic optimization. Chapter 3 proposes general scheduling model for microgrid and Chapter 4 discusses the carbon emission co-optimized microgrid scheduling formulation. In Chapter 5, the demand side management model for microgrid is proposed and solved. Chapter 6 presents the optimal medium-term operation portfolio for microgrid. Finally, conclusions and future works are discussed in Chapter 7. The nomenclatures of the mathematical formulations are presented in the Appendix A and Appendix B.

Chapter 2

Modeling and Decision Making under Uncertainty Environment

2.1 Uncertainty in microgrid operation

The uncertainties in microgrid operation mainly come from the random mismatch between forecasting results and actual realizations of renewable generation and load demand. In the bulk power system, uncertainties may also associate with unexpected contingency scenarios such as generation and transmission outage. However, considering the geographic scale and simple topology of microgrid, those factors are not considered in this dissertation. Therefore, in the proposed operation model, the uncertainties are assumed coming from the forecasting errors in renewable generations and demand side of microgrid.

Many researches have explored the probability distribution of forecasting errors. In [22], authors used statistical methods to evaluate the wind power and load forecast uncertainties. Both distribution fitting and empirical probability approaches were utilized in this paper. In [23], authors analyzed, modeled and compared the error distributions that arise from day-head wind power and load forecast systems that were used in three different ISOs in the United States. In [24], authors studied photovoltaic forecasting error models in different geographic and time scales. In [25], authors analyzed the frequency of occurrence of day-ahead wind power forecasting errors and used the results to generate an Auto Regressive Moving Average series (ARMA) to simulate the wind power production. In [26], authors proposed a heuristic simulation approach for wind power forecasting. In most of those literatures, the probability distribution of normalized day-ahead forecasting errors of wind, solar power production and load are described as a Gaussian distribution. However, some recent studies [20, 27, 28] shown that the forecasting error distribution of wind, solar power forecasting and load forecasting fit

better on leptokurtic distributions. In this dissertation, the normalized forecasting error distribution are assumed to follow multivariate Gaussian distribution since it would be more conservative from operation point of view to overly consider the uncertainty and variance in the optimization.

In the application of microgrid DSM operation, the uncertainties also come from the randomness in the price responsive patterns of the demand side. In [29], authors analyzed the price elasticity estimation for different pricing programs in multiple sectors. In [30], authors used the Electricity Market Complex Adaptive System (EMCAS) to simulate consumers' price elasticity of demand. In [31], authors developed a tool to estimate the price elasticity using data from dynamic pricing pilots with different pricing programs. Elasticity values are derived from an augmented Constant Elasticity of Substitution model. In [32], authors conducted multiple pricing experiments for household consumers to estimate their price responsive patterns. Similar experiment was also done by [33] for South Australia. From the literatures, it can be summarized that estimation of price responsive pattern, or the price elasticity of the demand side, highly depends on the end-users' marginal utility and opportunity cost. Consequently, the price elasticity is a time-variant function. For example it could change significantly between peak and off-peak hours [33]. In this dissertation, the probability distribution of price elasticity for microgrid loads on each operation period is assumed to follow a uniform distribution to address the estimation error for the price responsiveness. And the mean value of the uniform distribution forms a time-variance function.

2.2 Decision Making under Uncertainty Environment

As discussed in the previous section, there are numbers of uncertainties associated with microgrid operation. Therefore, the decision making strategy under uncertainty environment becomes critical for microgrid to achieve an economic and

environmental-friendly operation. There are multiple approaches that are commonly used for decision making under uncertainty, as summarized in the following [34].

2.2.1 Worst-case Optimization Approaches

This type of approach makes decisions to hedge against the worst-case outcome. In such type of approaches, the optimal operation decisions are supposed to achieve the optimal objective function $G(x, \omega)$ under the most extreme scenario (assuming the realization of random parameter vector ω is the extreme case, i.e. worst-case scenario). The chosen decision x is obtained by solving the following optimization problem.

$$\underset{x \in X}{Max}\left\{\underset{\omega \in \Omega}{Min}\ G(x, \omega)\right\} \tag{2.1}$$

2.2.2 Deterministic Optimization Approaches

This type of approach makes decisions based on the expected realization of random parameter vector ω. In such a way, the problem is converted to a typical optimization one with no uncertainties, as shown in the following.

$$\underset{x \in X}{Max}\left\{G(x, E(\omega))\right\} \tag{2.2}$$

The deterministic approach is one of the most commonly used decision making methods. For example, most of the current unit commitment algorithms are using the deterministic forecasting results for the uncertain parameters such as wind and hydro power generations. Those deterministic forecasting results are the expected realization for those random parameters.

2.2.3 Stochastic Optimization Approaches

This type of approach makes decisions to optimize the expected value of objective function $G(x,\omega)$ based on the probability distribution of random parameter vector ω. The chosen decision x is obtained by solving the optimization problem below.

$$\underset{x \in X}{Max}\left\{E\left(G\left(x,\omega\right)\right)\right\} \tag{2.3}$$

One of the basic optimization approaches when uncertainties involved is to maximize/minimize the expected objective function. Although the computational burden for the solving process might be increased depending on the chosen solving method, this kind of optimization approach does not introduce more complex model topology.

According to the Jensen's inequality, it is worth to mention that the objective function of the deterministic optimization (2.2) is biased upward relative to the objective function of the stochastic optimization formulation (2.3). The difference between those two approaches is the value of perfect information.

2.2.4 Probabilistic Constrained Optimization Approaches

This type of approach makes decisions to optimize the objective function $G(x, \omega)$ with a group of probabilistic constraints. The chosen decision x is obtained by solving the optimization problem shown in the following.

$$\begin{aligned} &\underset{x \in X}{Max}\left\{G\left(x,\omega\right)\right\} \\ &s.t.\ \Pr\left\{f_j\left(x,\omega\right) \le 0,\ j \in J\right\} \ge p \end{aligned} \tag{2.4}$$

This approach reflects the point that for a given decision, statistical hypothesis that $f_j\left(x,\omega\right) \le 0$ is not necessary true for all the scenarios. As long as the probability of this statistical hypothesis is satisfied is larger than certain threshold, the decision would be treated as feasible solution. These approaches are typically applied for the optimization problems when high level of uncertainty is involved and reliability is a critical issue.

2.3 Summary

There are a large amount of uncertainties involved in the microgrid operation decision making processes. Instead of using the conventional deterministic approach,

different decision making approaches should to be used to address those stochastic parameters in those optimization problems. In this dissertation, both stochastic optimization approach and probability constrained optimization approach are utilized to handle the uncertainties in the microgrid operation. Also, the corresponding deterministic formulations are also presented to model the original problem.

Chapter 3

Microgrid Generation Scheduling under Uncertainty Environment

As an important entity to implement renewable generation technologies combined with conventional fossil-fuel based generators and ESS, microgrid is expected to operate optimally to minimize the use of fossil fuel. Therefore, the optimal generation scheduling under a stochastic environment is the primary operation problem for microgrid.

3.1 Literature Review

The economic generation scheduling for microgrid has been investigated by numbers of research papers. In [35], authors presented an optimal power sharing model among distributed generators in a microgrid. In [36], authors conducted a long-term operation optimization for an experimental microgrid based on an estimated profile of renewable generation. In [37], authors presented a microgrid economic operation model based 1-day-ahead power forecasting. In [38], authors presented an optimal operation model of a community-based microgrid. In [39], authors performed a optimization operation analysis for a Combined Heat and Power (CHP) microgrid. In [40], authors put forward a multi-objective optimization model for a radial CHP microgrid. In [41], authors presented a niching evolutionary algorithm to solve the operation scheduling of a microgrid. Most of those researches were conducted based on deterministic renewable generation profile. Due to the stochastic nature of renewable energy and microgrid demand, the forecasting error from those deterministic profiles may result in a non-economic operation or other unintended consequences.

The stochastic nature of wind power has been taken into consideration in some transmission-level wind generation integration studies. In [42], Meibom *et al.* considered the forecasting error by using hourly-based scenario tree model. In [43], Pappala *et al.*

used a particle swarm optimization (PSO) based operation planning. In [44], Saber *et al.* presented a PSO and 5-scenario based unit commitment model. In [45], Hargreaves *et al.* combined Markov chain and dynamic programming to achieve a stochastic unit commitment model. However, those studies did not fully consider the unique characteristics of microgrid, thus the proposed approaches might not be applicable to microgrid operation. In this dissertation, a stochastic generation scheduling scheme for islanded microgrid is proposed. Compared with grid-connected microgrid, the generation scheduling for islanded microgrid is more important since all the loads need to be balanced by the local generation. To address the uncertainties associated with the microgrid generation scheduling operation, Probabilistic Constrained Stochastic Programming (PCSP) and Sample Average Approximation (SAA) model are quantitatively consider the randomness.

3.2 Mathematical Formulation

3.2.1 Deterministic Problem Formulation

The objective function of the deterministic microgrid generation scheduling problem can be formulated to minimize the overall operation cost over the entire scheduling horizon. The operation cost is composed of four parts: start-up cost, shut-down cost, no-load operation cost, and incremental fuel cost. This optimization formulation can be modeled as follows:

$$Min \sum_{t\in T}\sum_{i\in I}\left[SU_i u_{i,t} + SD_i v_{i,t} + O_i o_{i,t} + C_i p_{i,t} \right] \tag{3.1}$$

Subject to

$$P_{i,\min} o_{i,t} \le p_{i,t} \le P_{i,\max} o_{i,t} \quad \left(\forall i \in I, t \in T\right) \tag{3.2}$$

$$-o_{i,t-1} + o_{i,t} - o_{i,k} \le 0 \quad \left(2 \le k-(t-1) \le MU_i, \forall i \in I, t \in T\right) \tag{3.3}$$

$$o_{i,t-1} - o_{i,t} + o_{i,k} \le 1 \left(2 \le k-(t-1) \le MD_i, \forall i \in I, t \in T\right) \tag{3.4}$$

$$-o_{i,t-1}+o_{i,t}-u_{i,t}\le 0 \quad (\forall i\in I, t\in T) \tag{3.5}$$

$$o_{i,t-1}-o_{i,t}-v_{i,t}\le 0 \quad (\forall i\in I, t\in T) \tag{3.6}$$

$$p_{i,t}-p_{i,t-1}\le (2-o_{i,t-1}-o_{i,t})P_{i,\min}+(1+o_{i,t-1}-o_{i,t})RU_i \quad (\forall i\in I, t\in T) \tag{3.7}$$

$$p_{i,t}-p_{i,t-1}\le (2-o_{i,t-1}-o_{i,t})P_{i,\min}+(1-o_{i,t-1}+o_{i,t})RD_i \quad (\forall i\in I, t\in T) \tag{3.8}$$

$$\sum_{i\in I}P_{i,\max}o_{i,t}+\eta_{Dischar}P_{\max}^{Dischar}+p_t^{Wind}+p_t^{Pv}\ge R_t+p_t^{Load} \quad (\forall t\in T) \tag{3.9}$$

$$0\le p_t^{Dischar}\le z_t P_{\max}^{Dischar} \quad (\forall t\in T) \tag{3.10}$$

$$0\le p_t^{Char}\le (1-z_t)P_{\max}^{Char} \quad (\forall t\in T) \tag{3.11}$$

$$E_{\min}^{Stor}\le E_t^{Stor}\le E_{\max}^{Stor} \quad (\forall t\in T) \tag{3.12}$$

$$E_t^{Stor}=E_{ini}^{Stor}-\sum_{l=1}^{t}(p_t^{Dischar}-p_t^{Char})\Delta t \quad (\forall t\in T) \tag{3.13}$$

$$E_{final}^{Stor}=E_{ini}^{Stor}-\sum_{t\in T}(p_t^{Dischar}-p_t^{Char})\Delta t \tag{3.14}$$

$$\begin{aligned}&\sum_{i\in I}p_{i,t}+p_t^{Dischar}-p_t^{Char}+p_t^{Wind}+p_t^{Pv}=\\&p_t^{Load}+(1-\eta_{Char})p_t^{Char}+(1-\eta_{Dischar})p_t^{Dischar} \quad (\forall t\in T)\end{aligned} \tag{3.15}$$

In the above formulation, the decision variables are the scheduled outputs of fossil-fuel generation units and ESS. The fossil fuel generators' capacity constraints are defined in (3.2). The minimum up and down time for each generator is formulated in (3.3)-(3.4). Ramping rate constraints are defined in (3.5)-(3.8). The system spinning reserve constraint is defined in (3.9). The ESS of microgrid is modeled in (3.10)-(3.14). The maximum charging and discharging power is defined in (3.10)-(3.11). The capacity constraints of ESS are defined in (3.12)-(3.14). The power balance is constrained by (3.15), considering the charging/discharging losses of ESS. It should be noted that the transmission related constraints and losses are neglected in this microgrid operation

scheduling model due to the small geographical size of microgrid. Also, the contingency constraints are not included considering the fewer number of components and simpler topology of microgrid.

3.2.2 Stochastic Optimization Formulation

In the deterministic formulation, the wind power generation, solar power generation, and system demand during the operation horizon are considered as deterministic parameters based on the assumption that there is no forecasting error for all those predicted results. However, this is not the case in real operation conditions. The stochastic nature of renewable generations and system demand would make the actual realizations of those parameters random values which follow probability distributions [26]. To take those random parameters into consideration, the deterministic objective function (3.1) is replaced by a two-stage stochastic programming formulation [34] as shown in the following.

$$\begin{aligned} Min \sum_{t\in T}\sum_{i\in I}\left[SU_i u_{i,t} + SD_i v_{i,t} + O_i o_{i,t} + C_i p_{i,t} \right] \\ +\sum_{t\in T} \lambda_t E\left[V_t\left(p_{i,t}, p_t^{Dischar}, p_t^{Char}, \xi \right) \right] \end{aligned} \tag{3.16}$$

As shown in (3.16), the objective function contains two parts. The first stage cost, which is composed of the generation fuel cost, is the same as the deterministic formulation. The second stage cost indicates the penalty cost λ_t for the unserved load caused by over-estimation of renewable generations or under-estimation of microgrid system demand. The penalty factor represents the value of lost load (VoLL) [46, 47] for the microgrid at operation period t. In this formulation, the second stage cost is an expected value based on the probability distribution of random parameters. Considering the probability distributions are continuous [25, 26], it is difficult to analytically address those uncertainties. To handle this difficulty, Sample Average Approximation (SAA)

method is applied to generate a certain number of scenarios to represent the probability distribution of random parameters [48]. Therefore, the objective function (3.16) can be replaced by its approximation form.

$$\begin{aligned} &Min \sum_{t\in T}\sum_{i\in I}\left[SU_i u_{i,t} + SD_i v_{i,t} + O_i o_{i,t} + C_i p_{i,t} \right] \\ &+\frac{1}{N}\sum_{s\in S}\sum_{t\in T}\lambda_t V_{t,s}\left(p_{i,t}, p_t^{Dischar}, p_t^{Char}, \xi_{t,s} \right) \end{aligned} \tag{3.17}$$

In this formulation, the scenario set S has N realizations of the random vector ξ. It has been proved by multiple studies that the optimal solution of (3.17) will converge to its true counterpart (3.16) if a sufficiently large number of scenarios are accounted [34]. In the SAA formulation, the deterministic power balance constraints (3.15) can be replaced by the penalty cost of the unserved demand as shown in the following.

$$V_{t,s} = Max\left\{0, \Delta p_{t,s}\right\} \quad \left(\forall t \in T, s \in S\right) \tag{3.18}$$

$$\begin{aligned} \Delta p_{t,s} &= p_{t,s}^{Load} + \left(1-\eta_{Char}\right) p_t^{Char} + \left(1-\eta_{Dischar}\right) p_t^{Dischar} \\ &-\sum_{i\in I} p_{i,t} - p_t^{Dischar} + p_t^{Char} - p_{t,s}^{Wind} - p_{t,s}^{Pv} \quad \left(\forall t \in T, s \in S\right) \end{aligned} \tag{3.19}$$

3.2.3 Probabilistic Constrained Formulation

The SAA formulation discussed above takes the uncertainties in the microgrid operation scheduling into consideration by using the second stage penalty cost. The operation scheduling decision can be optimal if the estimation of VoLL is accurate on each operation period. However, it may be difficult to achieve a precise assessment for the VoLL especially when the composition of microgrid load is diversified. To overcome this drawback, this dissertation proposes a probabilistic constrained approach to optimize the operation scheduling of microgrid while restraining the risk of insufficient scheduled generation at certain level.

The probabilistic constrained stochastic optimization generally has a constraint which is bounded a conditional probability of a certain event. Instead of concentrating on

the expected value, this type of formulation enforces the probability of realization of the particular event. Based on this principle, a probabilistic constraint can be imposed on the microgrid operation as shown in the following.

$$\Pr\left\{\begin{array}{l}\sum_{i\in I} p_{i,t} + p_t^{Dischar} - p_t^{Char} + p_t^{Wind} + p_t^{Pv} \geq \\ p_t^{Load} + \left(1-\eta_{Char}\right) p_t^{Char} + \left(1-\eta_{Dischar}\right) p_t^{Dischar}\end{array}\right\} \geq 1\text{-}\, r \quad \left(\forall t \in T\right) \tag{3.20}$$

As demonstrated in (3.20), the probability that the DERs outputs satisfy the microgrid load on each operation period should be at least 1-*r*. In (3.20), *r* is defined as the operation risk for each operation period. $p_{i,t}$, $p_t^{Dischar}$ and p_t^{Char} are the decision variables. p_t^{Wind} , p_t^{Pv} and p_t^{Load} are considered as random parameters. Since the level of risk in (3.20) is based on each operation period, this type of constraints is treated as separate probabilistic constraints (SPC) in this chapter.

If the microgrid operator wants to guarantee a certain level of security over the entire operation horizon, another type of probabilistic constraint could be defined as the following.

$$\Pr\left\{\begin{array}{ll}\sum_{i\in I} p_{i,t} + p_t^{Dischar} - p_t^{Char} + p_t^{Wind} + p_t^{Pv} \geq & \\ p_t^{Load} + \left(1-\eta_{Char}\right) p_t^{Char} + \left(1-\eta_{Dischar}\right) p_t^{Dischar} & \left(\forall t \in T\right)\end{array}\right\} \geq 1\text{-}\, r \tag{3.21}$$

Note that the probability in (3.21) is actually a joint probability over the entire operation horizon. Therefore this type of constraints is considered as joint probabilistic constraints (JPC) in this chapter.

In the probabilistic constrained formulation, the objective function is the same as deterministic formulation and constraints (3.2)-(3.14) are also applicable. The power balance constraint is replaced by (3.20) or (3.21), for SPC and JPC formulation respectively.

3.3 Solution Method

To solve the stochastic problem formulations discussed above, the general principle is to convert stochastic models into deterministic problems. To achieve this conversion, the first step is modeling the uncertainties in microgrid operation. One of the challenges for uncertainty modeling is to find a relatively small amount of samples to properly represent the actual distribution of forecasting errors. The Monte Carlo Simulation method is used to generate those scenarios. To reduce the variance of the sample outcomes, the Latin hypercube sampling (LHS) method is applied in this chapter [49].

3.3.1 SAA Model

After the scenarios generated by sampling techniques, combining all the constraints, the SAA formulation can be treated as a typical two-stage stochastic programming problem with recourse.

It should be noted the second stage problem described in (3.18) is a non-linear formulation. It can be rewritten as the following form.

$$\Delta p_{t,s}^{+} - \Delta p_{t,s}^{-} = p_{t,s}^{Load} + \left(1-\eta_{Char}\right) p_t^{Char} + \left(1-\eta_{Dischar}\right) p_t^{Dischar} - \sum_{i\in I} p_{i,t} - p_t^{Dischar} + p_t^{Char} - p_{t,s}^{Wind} - p_{t,s}^{Pv} \quad \left(\forall t \in T, s \in S\right) \tag{3.22}$$

$$0 \le \Delta p_{t,s}^{+} \le y_t \Delta p_{Max} \quad (\forall t \in T, s \in S) \tag{3.23}$$

$$0 \le \Delta p_{t,s}^{-} \le \left(1-y_t\right) \Delta p_{Max} \quad (\forall t \in T, s \in S) \tag{3.24}$$

Consequently, the objective function can be rewritten as shown below.

$$Min \sum_{t\in T}\sum_{i\in I}\left[SU_i u_{i,t} + SD_i v_{i,t} + O_i o_{i,t} + C_i\left(p_{i,t}\right)\right] + \frac{1}{N}\sum_{s\in S}\sum_{t\in T}\lambda_t \Delta p_{t,s}^{+} \tag{3.25}$$

In this way, the original two-stage programming problem can be converted to a large-scale linear programming problem, which can be solved by most commercial solvers.

3.3.2 Probabilistic Constrained Model

As for the probabilistic constrained model, the following two different formulations come with different solving approaches.

3.3.2.1 SPC Type Formulation

It is assumed that the day-ahead forecasting errors for wind, solar and microgrid load (i.e. $e_t^{Wind}, e_t^{Pv}, e_t^{Load}$) follow Gaussian distributions at operation period *t*:

$$e_t^{Wind} \sim N\left(0, \sigma_t^{Wind}\right) \tag{3.26}$$

$$e_t^{Pv} \sim N\left(0, \sigma_t^{Pv}\right) \tag{3.27}$$

$$e_t^{Load} \sim N\left(0, \sigma_t^{Load}\right) \tag{3.28}$$

Then the probability distributions of the actual realization of those random parameters can be described based on the deterministic forecasting results (i.e. $\mu_t^{Wind}, \mu_t^{Pv}, \mu_t^{Load}$) as shown in the following:

$$p_t^{Wind} \sim N\left(\mu_t^{Wind}, \sigma_t^{Wind}\right) \tag{3.29}$$

$$p_t^{Pv} \sim N\left(\mu_t^{Pv}, \sigma_t^{Pv}\right) \tag{3.30}$$

$$p_t^{Load} \sim N\left(\mu_t^{Load}, \sigma_t^{Load}\right) \tag{3.31}$$

Since the probability distributions of random parameters are multivariable Gaussian distributions, three independent random parameters (i.e. $p_t^{Wind}, p_t^{Pv}, p_t^{Load}$) can form a new variable β_t that also follow a Gaussian distribution during the same operation period.

$$\beta_t = \sum_{i \in I} p_{i,t} + \eta_{Dischar}\, p_t^{Dischar} - \left(2 - \eta_{Char}\right) p_t^{Char} + p_t^{Wind} + p_t^{Pv} - p_t^{Load} \quad \left(\forall t \in T\right) \tag{3.32}$$

$$\beta_t \sim N\left(\mu_t^o, \sigma_t^o\right) \tag{3.33}$$

Therefore, the original probabilistic constrained can be replaced by the following constrains.

$$\Pr\{\beta_t \geq 0\} \geq 1\text{-}\, r \quad (\forall t \in T) \tag{3.34}$$

According to the definition of multivariable Gaussian distribution, the mean μ_t^o and standard deviation σ_t^o of β_t could be calculated:

$$\mu_t^o = \sum_{i \in I} p_{i,t} + \eta_{Dischar}\, p_t^{Dischar} - (2 - \eta_{Char})\, p_t^{Char} + \mu_t^{Wind} + \mu_t^{Pv} - \mu_t^{Load} \tag{3.35}$$

$$\sigma_t^o = \sqrt{\left(\sigma_t^{Wind}\right)^2 + \left(\sigma_t^{Pv}\right)^2 + \left(\sigma_t^{Load}\right)^2} \tag{3.36}$$

It should be noted that the following variable follows a standard Gaussian distribution.

$$\frac{\beta_t - \mu_t^o}{\sigma_t^o} \sim N(0,1) \tag{3.37}$$

Also, $\beta_t \geq 0$ is equivalent to:

$$\frac{\beta_t - \mu_t^o}{\sigma_t^o} \geq -\frac{\mu_t^o}{\sigma_t^o} \tag{3.38}$$

Based on the properties of Gaussian distribution, the probabilistic constrain can be replaced by the following constrain.

$$\Pr\left\{\alpha_t \geq -\frac{\mu_t^o}{\sigma_t^o}\right\} \geq 1\text{-}\, r \quad \left(\forall t \in T,\ \alpha_t \sim N(0,1)\right) \tag{3.39}$$

Given the Cumulative Probability Function (CPF) of standard Gaussian distribution is known as $\phi(x)$, the probabilistic constraint can be converted to a deterministic constraint.

$$-\frac{\mu_t^o}{\sigma_t^o} \leq \phi^{-1}(r) \quad (\forall t \in T) \tag{3.40}$$

It can be observed that the original SPC constraints have been replaced by explicit constraints. Combined with all those constraints, the SPC formulation has been rewritten as a deterministic linear programming problem which can be solved by most of the commercial solvers.

3.3.2.2 JPC Type Formulation

It should be noted that the solving method of SPC type formulation is not applicable to JPC type problem. That is because JPC contains joint constraints whose CPF are difficult to be described explicitly. By applying sampling techniques, constraint (3.21) can be rewritten as shown in the following.

$$g_t = \sum_{i \in I} p_{i,t} + \eta_{Dischar}\, p_t^{Dischar} - \left(2 - \eta_{Char}\right) p_t^{Char} \quad \left(\forall t \in T\right) \tag{3.41}$$

$$h_{t,s} = p_{t,s}^{Load} - p_{t,s}^{Wind} - p_{t,s}^{Pv} \quad \left(\forall t \in T, s \in S\right) \tag{3.42}$$

$$g_t + h_{t,s} x_s \geq h_{t,s} \quad \left(\forall t \in T, s \in S\right) \tag{3.43}$$

$$\sum_{s \in S} x_s \leq rN \tag{3.44}$$

With (3.41)-(3.44), the JPC type problem is reformulated as mix integer programming model. However, the continuous relaxation of this formulation makes the computational requirement impracticably large even for a linear objective function [50, 51]. To speed up the solving process, the stronger JPC formulation can be constructed by adding tighter continuous relaxation gaps [52]. Without loss of generality, random vector h_t can be transformed to k_t which has all the elements of h_t sorted in a descending order.

$$k_t = \left[k_{t,1}, \ldots, k_{t,N}\right] \quad \left(k_{t,1} \geq k_{t,2} \geq \ldots \geq k_{t,N}\right) \tag{3.45}$$

After h_t is replaced by k_t, it can be noticed that $x_s = 1$ cannot be true for all $s = 1,\ldots,l+1$ in order to satisfy (3.44). Also, as long as there is one $x_s = 0$ for $s = 1,\ldots,l+1$, the following constraints would be redundant.

$$l = floor(rN) \tag{3.46}$$

$$g_t + h_{t,s} x_s \geq h_{t,s} \quad (\forall t \in T, s = l+1, \cdots, N) \tag{3.47}$$

Therefore, the original JCP formulation of (3.41)-(3.44) can be tightened by replacing (3.43) with the following constraints.

$$g_t + \sum_{s=1}^{l} \left(k_{t,s} - k_{t,s+1}\right) x_{[s]} \geq k_{t,1} \quad (\forall t \in T) \tag{3.48}$$

In (3.48), index [s] of $x_{[s]}$ means the index of $k_{t,s}$ in the original random vector h_t. In some papers constraints similar to (3.48) are called star-inequalities [51]. Combining those star-inequalities constraints, the JPC type formulation can be solved efficiently by commercial optimization solvers.

3.4 Numerical Study

In this section, a sample microgrid system is used to examine and compare the proposed stochastic models. All system modeling and solving algorithms are coded in Matlab and solved by CPLEX 12.5.1[53]. All experiments are run on a computer with AMD X6 CPU@2.70 GHz and 8 GB memory.

3.4.1 System Configuration

The experiment microgrid is composed of three fossil-fuel units, one energy storage system, one aggregated wind farm, one aggregated solar station, and loads, as shown in Figure 3-1. To illustrate the effects of different types of fossil-fuel units on the generation fuel cost, three different types of generators, which are Coal, Gas Steam and Combined Cycle Gas Turbine (CCGT), are assumed in this microgrid. The assumed

characteristics for fossil-fuel generators are scaled down from ERCOT scheduling data as shown in Table 3-1 and Table 3-2. The ESS data is depicted in Table 3-3. To achieve a neutral energy impact on the whole operation scheduling horizon, both final storage level and initial storage level of the ESS are set to 50%.

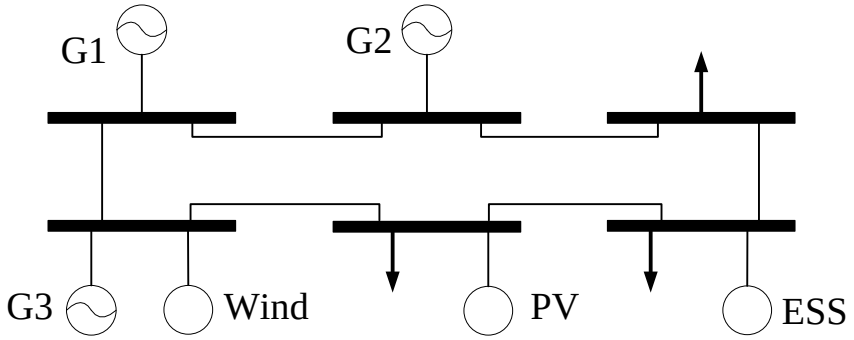

Figure 3-1 Experiment microgrid system

As mentioned in the above, the uncertainties in the microgrid day-ahead operation scheduling problem are modeled based on forecasting error distributions. In the simulation, the mean and standard deviation of the day-ahead forecasting data is based on recent research [20, 23, 27, 28], as shown in Table 3-4. It should be noted that the normalized standard deviation of the day-ahead forecasting error is the actual mismatch value divided by the nominal rating.

Table 3-1 Generator Operation Data

Unit	Fuel Type	Max/Min Output (MW)	Ramp Up/Down Rate (MW/h)	Min Up/Down Time (h)
G1	Coal	90/30	47/65	3/2
G2	Gas Steam	40/5	28/35	1/1
G3	CCGT	60/10	48/93	2/1

Table 3-2 Generator Fuel Data

Unit	Start-up Fuel Cost ($)	Shut-down Fuel Cost ($)	No-load Fuel Cost ($/h)	Marginal Heat Rate (MMBtu/MWh)	Fuel Price ($/MMBtu)
G1	28536	11849	1985	9.8	2.49
G2	5384	2941	857	11.9	4.51
G3	9375	3577	1162	5.4	4.51

Table 3-3 Energy Storage System Data

Storage Capacity (MWh)	Max Storage Level	Min Storage Level
100	90%	10%
Max Discharge Rate (MW)	Discharge Efficiency	Initial Storage Level
10	85%	50%
Max Charge Rate (MW)	Charge Efficiency	Final Storage Level
15	85%	50%

Table 3-4 Uncertainties in Microgrid Operation Scheduling

Type	Nominal Rating (MW)	Normalized Standard Deviation of Day-ahead Forecasting Error
Wind	75	11.90%
Solar	40	5.10%
Load	167.8	2.60%

3.4.2 SAA Approach

Based on the microgrid system configuration, the day-ahead operation schedule for the experiment microgrid is solved by SAA model with 50 scenarios. The penalty factor for the unserved load is assumed to be 9000$/MWh. The scheduling solution is shown in Figure 3-2.

Since the uncertainties of the operation scheduling in SAA formulation are accounted by the cost of unserved load, the penalty factor plays an important role in determining the total objective cost of the optimal scheduling solution. To illustrate the effect of the penalty factor on the objective cost, the SAA model is investigated with different penalty factors, as shown in Figure 3-3. It can be observed that the objective operation cost increased as the penalty factor increased. This is because a higher

penalty factor indicates that a higher penalty will be imposed if a certain amount of load cannot be served. Consequently, the SAA scheduling model would increase the scheduled generation to reduce the risk of unserved load. As a result, the objective operation cost will increase as the penalty factor increases. For a certain microgrid, the penalty factor in the SAA model should be determined by the value that local customers would like to pay for a reliable electricity service [54], which is known as VoLL.

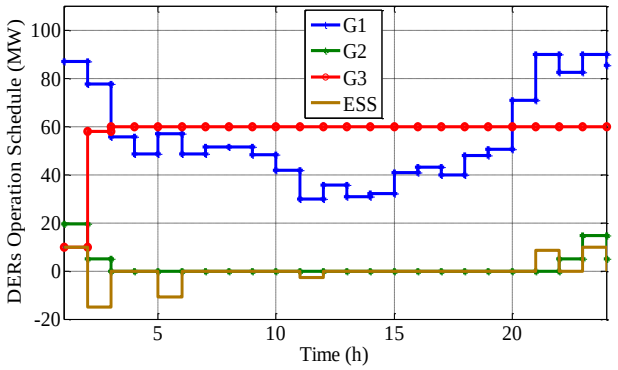

Figure 3-2 Operation schedule for DERs for SAA model

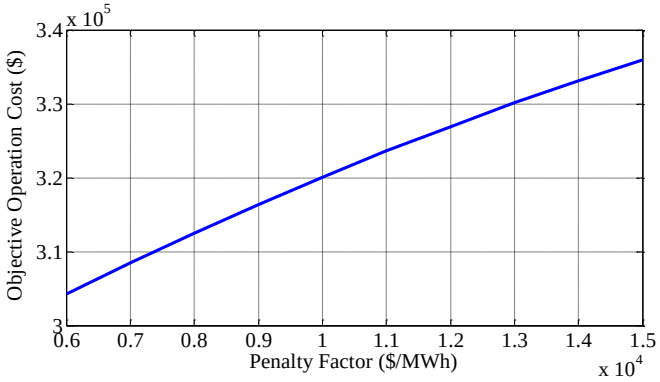

Figure 3-3 Operation schedule cost vs penalty factor for SAA model

3.4.3 SPC Approach

In the SPC model, the operation risk level is accounted for each operation period. Figure 3-4 presents the day-ahead operation schedule for the experiment microgrid solved by SPC model with r = 0.1.

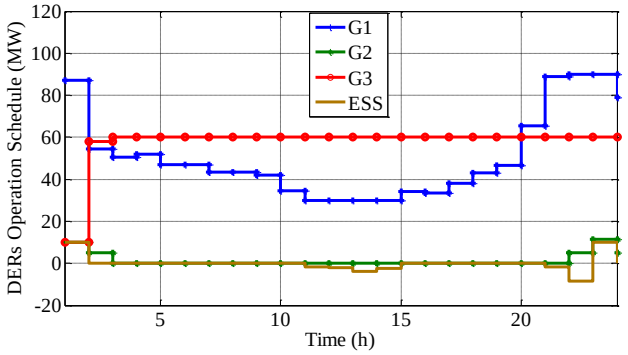

Figure 3-4 Operation schedule for DERs for SPC model (r = 0.1)

To investigate the effect of operation risk level on the total operation cost, the problem is solved by SPC model with different operation risks, and results are reported in Figure 3-5. It can be observed that objective operation cost is reduced as the operation risk level increased from 0.1 to 0.9. This is expected since a higher risk level in microgrid SPC model indicates there is a greater possibility that microgrid load will not be served by the scheduled DERs output. In other words, a higher operation risk level indicates that the operation schedule has a lower reliability. Therefore, it should be noted that the reduction of operation cost in SPC model comes at the expense of reducing the reliability of microgrid operation.

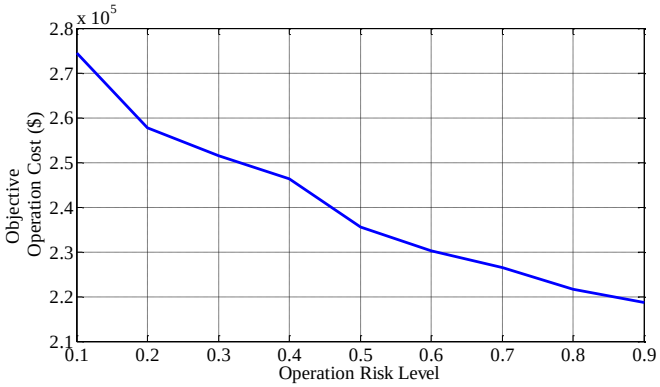

Figure 3-5 Objective operation cost vs risk for SPC model

It also should be noted that when the operation risk r equals 0.5, the SPC model is equivalent to the deterministic model. This is because the probability constraints of SPC model would impose the mean values of stochastic parameters if $r = 0.5$, which are equal to those corresponding parameters in the deterministic formulation.

3.4.4 JPC Approach

As discussed above, JPC formulation can be modeled as a mixed integer programming problem. Figure 3-6 presents the day-ahead microgrid operation schedule solved by JPC model with risk level $r = 0.1$ and 50 scenarios. The time resolution of operation schedule for all the fossil-fuel generators and ESS are hourly basis, as reported in the following.

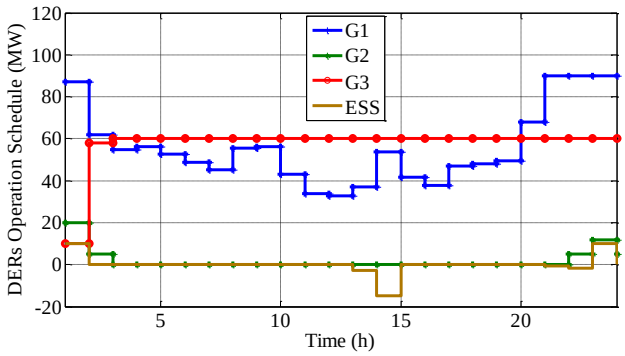

Figure 3-6 Operation schedule for DERs for JPC model ($r = 0.1$)

Figure 3-7 presents the optimal results solved by JPC model with different operation risk levels. Similar to the SPC model, the operation cost of JPC model is monotonically decreasing as the level of operation risk increases. The results imply that minimizing operation cost in JPC model may jeopardize the security of microgrid operation.

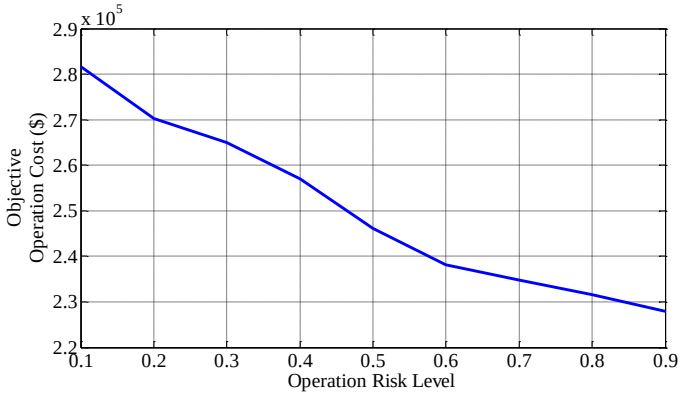

Figure 3-7 Objective operation cost vs risk for JPC model

3.4.5 Model Comparison

To illustrate the impact of the scenario number on the optimal solution of SAA model and JPC model (note that there is no scenario generation in SPC model, therefore it does not involve any scenario-related analysis for SPC model), the microgrid scheduling problem is solved by both models with different scenario number N. As presented in Figure 3-8, the objective operation cost of JPC model is always lower than the cost of SAA model when considering same amount of scenarios. This is because the SAA model tries to schedule the DERs operation to satisfy the microgrid load unless the marginal cost of serving additional load becomes larger than the VoLL. In contrast, the JPC model only guarantees a certain probability (i.e. $1\text{-}r$) that the microgrid load can be served by DERs. Another observation from Figure 3-8 is that JPC model converges to its true counterpart faster than SAA model as scenario number increases. This is because when the scenario number increases, the probability of extreme samples also increases. Those extreme scenarios (i.e. worst-case scenarios) have larger impacts on the operation cost of SAA model since it requires the operation schedule to satisfy the microgrid load in all the scenarios otherwise it gets a penalty based on the VoLL. Compared with that, the probability distribution of scenarios does not change

substantially when the number of scenarios increases. Consequently, the objective operation cost of JPC model is not affected as much as it is in the SAA model.

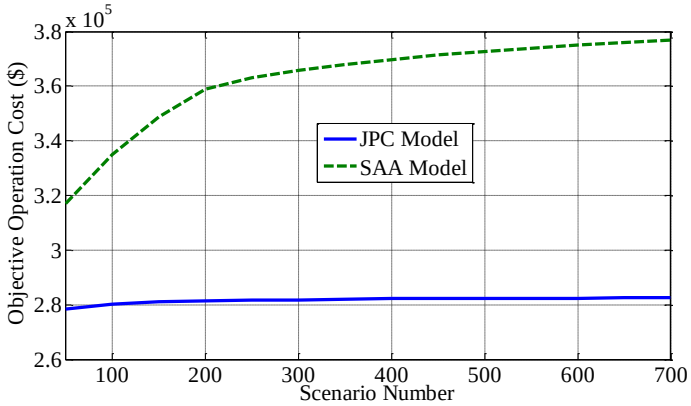

Figure 3-8 Objective operation cost of JPC model (r = 0.1) and SAA model (π = 9000$/MWh) at different scenario numbers

To further assess the impact of scenario number on SAA and JPC models, the scheduling problem is solved by both models 100 times with each particular scenario number. For each scenario number, the Kolmogorov-Smirnov (KS) test indicates that Gaussian distribution provides a good fit to the 100 run results. The standard deviation of 100-run results for each particular scenario number is compared in Figure 3-9. It can be observed that JPC model always has a smaller variance than SAA model when the same amount of scenarios are considered in the optimization. The reason is that JPC model is constrained by a probability, and the probability distribution of different times of sampling would not change significantly. In contrast, different times of sampling may result in different extreme scenarios. Those extreme scenarios have larger impacts on the objective value of SAA models, as explained above. Therefore, JPC model tends to have a smaller variance than SAA model.

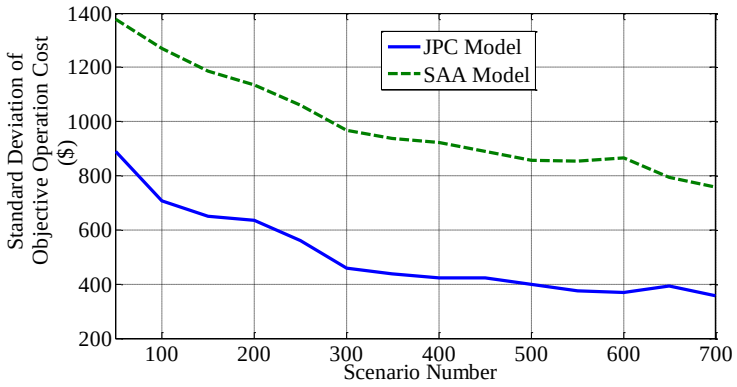

Figure 3-9 Standard deviation of 100-run optimal solutions for JPC model ($r = 0.1$) and SAA model

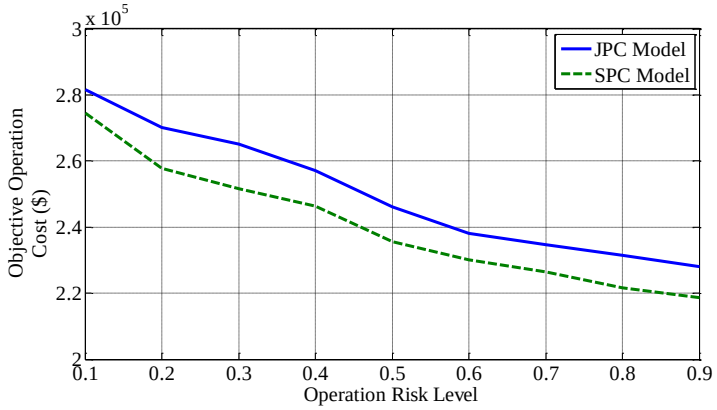

Figure 3-10 Objective Fuel Cost Comparison between JPC model and SPC model

Figure 3-10 presents a comparison between SPC model and JPC model under different operation risks. It can be observed that objective operation cost of JPC model is always higher than SPC model for the same operation risk level. This is reasonable since JPC model is defined by a stronger constraint that the operation schedule of DERs should satisfy for the entire operation horizon while SPC model is defined over each operation period. In other words, the feasible region of JPC model is a subset of SPC model's feasible region. Therefore, optimal operation schedule of JPC model has a

higher operation cost. It should also be noted that operation schedule of JPC model has a higher reliability than the one obtained by SPC model.

With all the results discussed above, the characteristics of SAA model, SPC model and JPC model are illustrated and compared. Among those three stochastic scheduling approaches, the SAA formulation has the highest reliability if the same level of randomness (same number of scenarios) is considered and proper VoLL is included. This is because the SAA model tries to satisfy the microgrid load in all scenarios unless the marginal cost of the DERs' scheduled operation is higher than the VoLL of microgrid local demand. Correspondingly, the operation cost of SAA model is the highest among those formulations. Another feature of SAA model is that the effectiveness of this approach highly depends on the estimation accuracy of VoLL. The estimation of VoLL for islanded microgrids could be easier than for bulk power systems, but it still depends on many factors such as the number of consumers, the composition of the system demand and the time of the interruption [54].

For probability constrained approaches, one of their major advantages is that the operation risk level can be dynamically adjusted by the operator. For example, r can be intentionally set to a smaller value if the microgrid operator knows that the reliability requirement for certain period of time is increased. As discussed above, solutions of JPC model usually have a higher reliability than SPC model solutions with the same r. However, JPC model also has greater operation cost as shown in Figure 3-10. Conversely, the SPC model has a unique feature in that that it can set the operation risk dynamically for the day-ahead operation schedule since its probability constraints can be set separately for each operation period. This can also benefit microgrid operation scheduling by increasing the reliability for critical periods and reducing generation fuel cost for other non-sensitive periods.

3.5 Summary

In this chapter, a stochastic day-ahead scheduling scheme is proposed to address uncertainties in microgrid operation. Both SAA and PCSP approaches are utilized for modeling the microgrid operation scheduling problem and three different stochastic models are presented in this chapter. The corresponding solution methods are developed and numerical case studies are conducted to compare those models. The results compare and illustrate characteristics of different models.

Chapter 4

Microgrid Generation Scheduling considering Carbon Emission under Uncertainty Environment

As the concerns of climate change are mounting, it is the responsibility of the entire society, including the power industry, to control and reduce the carbon emission. Many countries have proposed rules and regulations to lower GHG/carbon emissions [55, 56]. In March 2010, the EU committed to reducing its carbon emissions to 20% below 1990 levels by 2020 [57]. In June 2014, the U.S. Environmental Protection Agency (EPA) also released a long-anticipated proposal to reduce America's carbon dioxide emissions 30% from 2005 levels by 2030 [58]. Those facts offer the motivation for microgrid to achieve a low carbon emission operation. Meanwhile, as one of the most effective methods for carbon emissions reduction, implementing renewable generation technologies also bring uncertainties to microgrid operation. In this chapter, the microgrid generation scheduling co-optimized with carbon emission is studied and solved.

4.1 Literature Review

Many studies have been performed on bulk power systems to achieve a low carbon emission target. In [59], Muslu discussed the conflict nature between minimizing generation fuel cost and carbon emissions. In [60], Zhen *et al.* put forward a low-carbon co-optimization dispatch model considering carbon capture power plants. In [61], Norouzi *et al.* presented a multi-objective optimization model to achieve the Pareto solutions to consider both generation fuel cost and emission cost. In [62], Abido presented a particle swarm optimization based carbon/economic co-dispatch model. In [63], Wang *et al.* presented a day-ahead unit commitment model including carbon emission cost for a wind-coal intensive power system. In [64], Lu *et al.* proposed a cultural algorithm based scheduling model to achieve low carbon dispatch. Most of those greenhouse gas (GHG)

/carbon emission scheduling models are based on deterministic approaches. Due to the stochastic nature of renewable generation resources and system demand, the uncertainties in the operation scheduling may result in a non-optimal schedule or even jeopardize the security of system operation. In this chapter, a microgrid operation scheduling scheme is proposed to co-optimize the generation fuel cost and carbon emissions via a carbon emission price. Similar to Chapter 3, multiple stochastic optimization techniques are utilized to model and solve the proposed scheme.

4.2 Problem Formulation and Solving Method

4.2.1 Mathematical Formulation

The objective of the deterministic microgrid day-ahead carbon emission co-optimized scheduling problem can be formulated to minimize the overall operation cost over the entire scheduling horizon. Compared with the objective function in (3.1), the carbon emission co-optimized objective can be divided in two parts: generation fuel cost and carbon emission cost. The generation fuel cost part is similar to the conventional deterministic problem, which is shown in (3.1). The carbon emission cost can be induced by emission-related policies, such as carbon tax or carbon cap-and-trade mechanism [60, 65]. Thus the objective function can be modeled as shown in the following.

$$\begin{aligned} Min \sum_{t\in T}\sum_{i\in I}\left[SU_i u_{i,t} + SD_i v_{i,t} + O_i o_{i,t} + C_i p_{i,t} \right] \\ +\pi \sum_{t\in T}\sum_{i\in I}\left[SU_i^E u_{i,t} + SD_i^E v_{i,t} + O_i^E o_{i,t} + C_i^E p_{i,t} \right] \end{aligned} \tag{4.1}$$

In this formulation, the objective function contains the generation fuel cost and carbon emission cost. The start-up, shut-down, no-load operation and incremental operation cost are all associated with the carbon emission. The penalty factor π is the carbon emission price. Similar to the microgrid scheduling problem described in Chapter 3, the decision variables are the scheduled outputs of fossil-fuel units and ESS. The

constraints for this formulation are also the same with (3.2)-(3.15), which are defined for the microgrid scheduling problem in Chapter 3.

To address the uncertainties in the operation scheduling process, the car-emission co-optimized problem is also modeled via SAA approach. The stochastic parameters are considered in the formulation based on their probability distribution. Therefore, a stochastic programming based objective function is the presented as shown in the following.

$$\begin{aligned} &Min \sum_{t\in T}\sum_{i\in I}\left[SU_i u_{i,t} + SD_i v_{i,t} + O_i o_{i,t} + C_i p_{i,t}\right] \\ &+\pi\sum_{t\in T}\sum_{i\in I}\left[SU_i^E u_{i,t} + SD_i^E v_{i,t} + O_i^E o_{i,t} + C_i^E p_{i,t}\right] \\ &+\sum_{t\in T}\lambda_t E\left[V_t\left(p_{i,t}, p_t^{Dischar}, p_t^{Char}, \xi\right)\right] \end{aligned} \tag{4.2}$$

Applying Monte Carlo simulation, the continuous probability distribution can be discretized. Then the objective function (4.2) can be replaced by its approximation form.

$$\begin{aligned} &Min \sum_{t\in T}\sum_{i\in I}\left[SU_i u_{i,t} + SD_i v_{i,t} + O_i o_{i,t} + C_i p_{i,t}\right] \\ &+\pi\sum_{t\in T}\sum_{i\in I}\left[SU_i^E u_{i,t} + SD_i^E v_{i,t} + O_i^E o_{i,t} + C_i^E p_{i,t}\right] \\ &+\frac{1}{N}\sum_{s\in S}\sum_{t\in T}\lambda_t V_{t,s}\left(p_{i,t}, p_t^{Dischar}, p_t^{Char}, \xi_{t,s}\right) \end{aligned} \tag{4.3}$$

In the above formulation, the violation $V_{t,s}$ is defined the same way which is described in (3.18) and (3.19).

Meanwhile, the probability constrained formulations are also proposed in this chapter. If the power-balance constraint is replaced by (4.4) and (4.5), the SPC and JPC formulation for carbon-emission co-optimization can be established respectively.

$$\Pr\left\{\begin{array}{l}\sum_{i\in I} p_{i,t} + p_t^{Dischar} - p_t^{Char} + p_t^{Wind} + p_t^{Pv} \geq \\ p_t^{Load} + \left(1-\eta_{Char}\right) p_t^{Char} + \left(1-\eta_{Dischar}\right) p_t^{Dischar}\end{array}\right\} \geq 1\text{-}\, r \quad \left(\forall t \in T\right) \tag{4.4}$$

$$\Pr\left\{\begin{array}{l}\sum_{i\in I} p_{i,t} + p_t^{Dischar} - p_t^{Char} + p_t^{Wind} + p_t^{Pv} \geq \\ p_t^{Load} + \left(1-\eta_{Char}\right) p_t^{Char} + \left(1-\eta_{Dischar}\right) p_t^{Dischar} \quad \left(\forall t \in T\right)\end{array}\right\} \geq 1\text{-}\, r \tag{4.5}$$

4.2.2 Solution Method

The principle for solving those stochastic formulations is converting the random parts to deterministic realizations. Similar to the microgrid operation scheduling problem in Chapter 3, the randomness in carbon-emission co-optimized problem is characterized by scenarios generated by Monte Carlo simulations. The solving approaches for each individual stochastic formulation have already been discussed in Chapter 3.

4.3 Numerical Study

A sample microgrid is utilized to verify and illustrate the proposed stochastic microgrid operation scheme to co-optimize the carbon emission and generation fuel cost. The configuration information of the sample microgrid is depicted in Table 3-1 to Table 3-4 and the schematic of microgrid is shown in Figure 3-1. To analysis the carbon emission of the generation mix of this sample microgrid, the emission data is listed in Table 4-1.

Table 4-1 Generator Emission Data

Unit	Start-up CO_2 Emission (ton)	Shut-down CO_2 Emission (ton)	Non-Load CO_2 Emission (ton/h)	Marginal CO2 Emission (ton/MMBtu)
G1	1375	746	125	0.1085
G2	91	59	11	0.0545
G3	107	68	14	0.0561

4.3.1 SAA Approach

To illustrate the impact of carbon emission price on actual carbon emissions, the problem formulation is solved with different carbon emission prices, as shown in Figure 4-1. The corresponding generation fuel cost is also shown in that figure for comparison purpose.

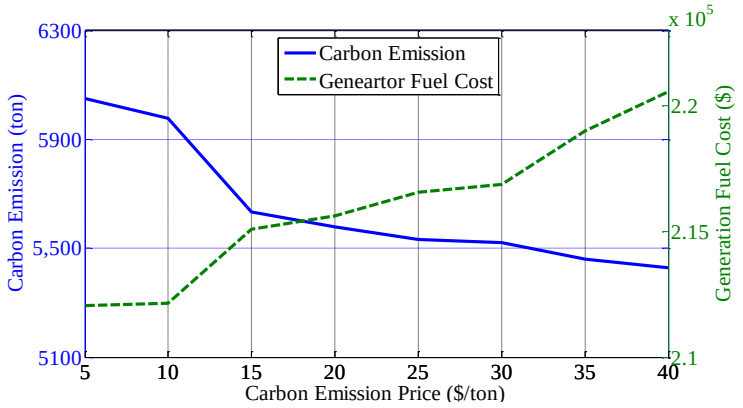

Figure 4-1 Carbon emission and generation fuel cost vs carbon emission price for SAA model

As shown in Figure 4-1, the carbon emissions are reduced when the carbon emission price increases. The corresponding generation fuel cost also increases. This is because minimizing carbon emissions and minimizing generation fuel cost are conflicting objectives for the microgrid operation scheduling problem [66]. In the proposed SAA formulation, those two conflicting objectives are co-optimized via the carbon emission price. As the carbon emission price increases, the weight of minimizing carbon emission objective increases. As a result, carbon emissions of the optimal operation schedule are reduced when the generation fuel cost increases.

4.3.2 SPC Approach

The SPC model are also solved with multiple carbon emission price to illustrate the trade-off relations between carbon emission and generation fuel cost, as shown in Figure 4-2. Concurrent with previous results, it can be observed that carbon emissions are reduced as the corresponding generation fuel cost increases along with the carbon emission price.

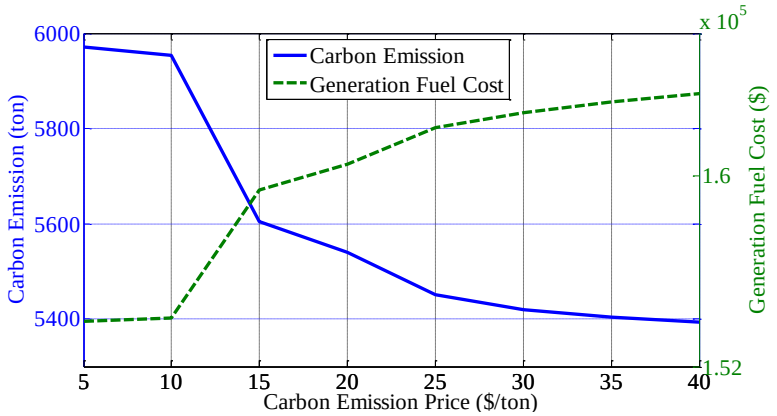

Figure 4-2 Carbon emission and generation fuel cost vs carbon emission price for SPC model (r = 0.1)

To explore the impact of operation risk level on the carbon emission, the SPC formulation is solved with different operation risk levels, as shown in Figure 4-3. As expected, the carbon emission level decreases as the required operation risk level increases. This can be explained that higher risk level indicates the larger possibility that the load will not be fully served by the scheduled microgrid. Consequently, the scheduled generation produces less carbon emission.

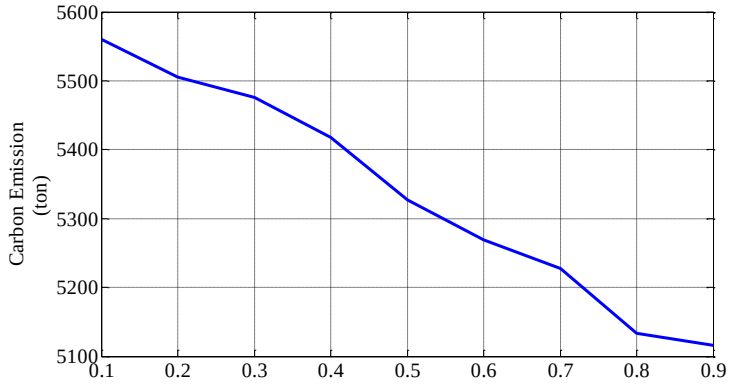

Figure 4-3 Carbon emission vs risk for SPC model

4.3.3 JPC Approach

Similar to the SPC model, JPC formulation is also solved with multiple carbon emission price and results are reported in Figure 4-4.

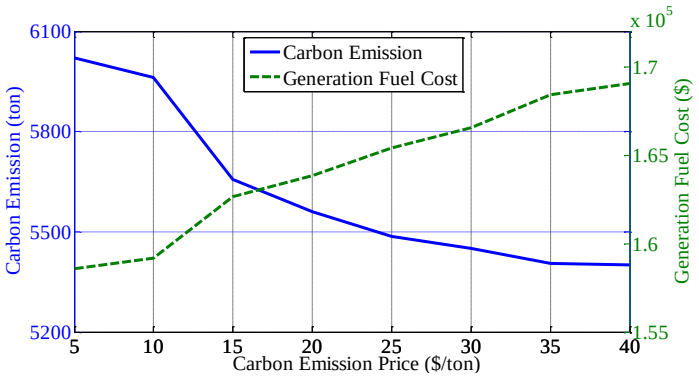

Figure 4-4 Carbon emission and generation fuel cost vs carbon emission price for JPC model (r = 0.1)

Meanwhile, the JPC formulation is solved with different operation risk levels, as shown in Figure 4-5. Similar result is achieved that the carbon emission level decreases as the required operation risk level increases.

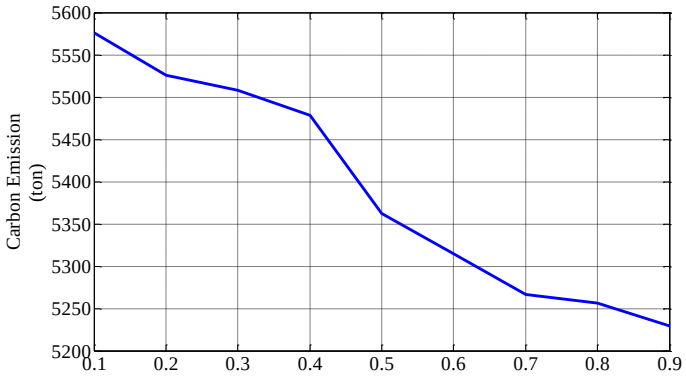

Figure 4-5 Carbon emission vs risk for JPC model

4.3.4 Model Comparison

To compare two PCSP approaches, Figure 4-6 is presented to show the carbon emission difference with the same operation risk level setting. It can be observed that JPC formulation has a higher emission amount than that of SPC formulation. This is expected because the feasible set for JPC is subset of SPC's thus JPC is stronger constraint, as summarized in Chapter 3. In other words, the schedule solution of JPC formulation is more reliable compared with that of SPC model.

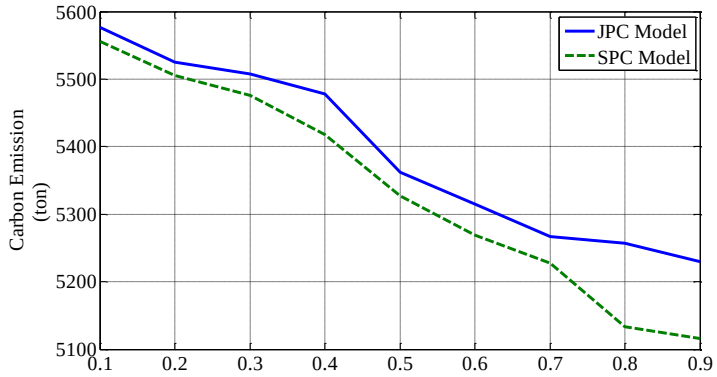

Figure 4-6 Carbon emission comparison between JPC model and SPC model

4.4 Summary

In this chapter, the microgrid operation scheduling problem is co-optimized with carbon emission. Three stochastic formulations are proposed to address the uncertainties in this process. Numerical results illustrates the trade-off among carbon emission, generation fuel cost and operation risks.

Chapter 5

Microgrid Demand Side Management under Uncertainty Environment

The intermittence nature of distributed renewable generation presents significant challenges for microgrid operation. The variable pattern of renewable generation, especially on-shore wind generation, sometimes does not match with typical daily load profiles [15, 67]. During the peak demand, the output of wind power may be low while the wind power may need to be curtailed during the off-peak hours. The conventional solutions are using marginal cost fossil-fuel units or integrating more energy storage to balance the generation and demand in the microgrid [16]. However, both approaches may result in a high environmental and financial cost.

Considering the deployment of advanced meter infrastructure (AMI) and delicate communication system, it provides an alternative solution for microgrid to balance the generation and demand by optimally managing the demand side. Generally, the demand side management (DSM) can be divided into two types: incentive based program and pricing based program [68]. Incentive based programs include direct load control programs and interruptible load programs. System operator secures the curtailable capacity prior to the operation period. Participating customers receive a capacity payment for selling the interruptible capacity and an energy payment if the demand response is deployed upon system operator's request. Incentive based DSM program can be used for frequency regulation and peak demand shaving. Consequently, extra capacity cost required by system operation can be reduced by implementing these types of programs. Pricing based program is using the dynamic price signal to affect the consumption pattern based on the end-users' price responsiveness. The time-variant pricing program offers higher rates during peak periods and lower rates during off-peak periods. The responsive loads can be adjusted in both direction based on the system real-time price and their

elasticity. In this way, the demand peak can be shaved and demand can be optimally shifted based on the system generation cost with little sacrifice of consumers' utility [69].

Compared with conventional bulk power system, microgrid, with its technological and regulatory innovation of scale and structure, has advantages to encourage its customers to participate in pricing based DSM programs. With AMI and smart control system installed, it is also easier for microgrid to learn the responsive pattern (i.e. price elasticity) of different groups of loads at different operation periods [70].

5.1 Literature Review

Several researches have explored the application of DSM programs in microgrid. Palma-Behnke *et al*. [71] proposed an energy management system (EMS) based rolling horizon strategy and online signals to manage the microgrid demand. Adika *et al*. [72] used a consumer appliance scheduling model to optimally rescheduling the demand in a residential microgrid. Gouveia *et al*. [73] utilized direct load control strategies to improve microgrid resilience following islanding operation. Pourmousavi *et al*. [74] presented a demand management model for frequency regulation purpose by directly manipulating loads. Wang *et al*. [75] proposed a demand response strategy to smooth the tie-line between microgrid and utility grid by optimally coordinate the thermal appliance and energy storage. Tasdighi *et al*. [76] coordinated the thermal and electrical loads directly to optimize the operation of a CHP microgrid. Farzan *et al*. [77] and Shahidehpour *et al*. [78] discussed the capability of grid-tie microgrids participating incentive based DSM programs offered bulk power system operator.

Most of the microgrid DSM approaches focused on incentive based DSM programs. This kind of applications requires the capability of directly control of end-users' appliances. To achieve such kind of capability, microgrid needs to equip with an energy management system which is capable of directly controlling and metering all participating

appliances. The installation of all the control and meter devices can be costly. Besides, it also involves agreements signed by both customers and microgrid operator to permit this kind intrusive load control, which is not desirable from system operation point of view.

In this chapter, a stochastic internal pricing based demand side management (IPDSM) model is presented. Instead of controlling end-users' loads directly, this model proposes a dynamic internal pricing strategy to optimally reschedule the microgrid demand based on customers' price responsive patterns. Combining unit commitment and DSM, the model provides an optimal operation schedule and price policy for next day operation. In this way, both peak shaving and load shifting can be achieved so that the utilization factor of renewable energy can be improved and start-up of additional units can be avoided. Incentives for implementing this IPDSM model for both generation resources and consumers are also provided by incorporating generation resource revenue constraints and bill protection constraints. The price responsiveness of the microgrid demand is addressed by multiple load groups thus the financial equality among different types of consumers with different price response patterns can be guaranteed. To address the stochastic nature of uncertainties of consumers' responsive patterns and renewable energy generation, stochastic optimization techniques are applied to model and solve this problem.

5.2 Model Description

In the proposed microgrid IPDSM model, the objective is to minimize the microgrid total operation cost while satisfy all the constraints from both demand side and operator side. In this model, microgrid operator is assumed to run the model based on updated renewable generation forecasting and estimated consumers' responsive patterns to achieve the optimal pricing policy. This pricing policy should be published to all the end-user customers through microgrid communication systems prior to the next

day's operation. Assuming there are sufficient numbers of participated consumers, the total consumption adjustment based on the published pricing policy can be projected by the estimated price responsive patterns (i.e. price elasticity).

To model the price responsive patterns, microgrid loads are categorized into *J* load groups according to load owners' price responsive patterns. For example, households with similar incomes and consumption habits might be aggregated into the same load group if their responses to price change are similar. The price elasticity for a certain load group is a function of time. Similar to the forecasting of renewable energy generation, the price elasticity can be dynamically estimated prior to the next day's operation [79]. Through this approach, the price responsive patterns of different load groups can be addressed separately as time-variant parameters in the microgrid IPDSM model.

The optimal dynamic pricing policy is obtained based on the flat base price and base load profiles. In the presented model, the flat base price is calculated based on long term microgrid operation cost which also includes a recovery rate for capital investment and other types of costs. The base load profile is formed by forecasted demand of each given load group under the flat base price policy. After the dynamic internal pricing policy achieved from the IPDSM model is published, each load group would adjust their consumption pattern according to the published price policy. Consequently, the optimal demand side management can be achieved.

5.3 Mathematical Formulation

5.3.1 Deterministic IPDSM Model

In deterministic IPDSM model, the objective function is formulated to minimize the operation cost for the whole operation horizon, which is the same with (3.1) as shown in Chapter 3. Also the IPDSM model shared the generation capacity constraints,

minimum up and down time constraints, units ramping rate constraints, system reserve constraints, ESS related constraints, renewable energy generation constraints and system power balance constraint as shown in (3.2) - (3.15).

As the dynamic pricing policy is published, the demand side would response to the price change. The responsive pattern of load group *j* at operation period *t* can be modeled by its corresponding price elasticity [80], which is shown in (5.1).

$$p_{j,t}^{Load} = p_{j,t,base}^{Load} + \Delta\pi_t \varepsilon_{j,t}^{Load} / \pi_{base} \quad (\forall j \in J, t \in T) \tag{5.1}$$

To encourage the adoption of the proposed dynamic internal pricing strategy on the consumer end, additional constraints for bill protection mechanism [81] are implemented in the model. With those constraints, even if an average consumer (i.e. the consumption pattern is similar with its load group's profile) fails to response to dynamic price change, there would be no increase in his/her bill. The mathematical formulation of those constraints is shown in the following.

$$\sum_{t \in T} p_{j,t,base}^{Load} (\pi_{base} + \Delta\pi_t) \leq \sum_{t \in T} p_{j,t,base}^{Load} \pi_{base} \quad (\forall j \in J) \tag{5.2}$$

Moreover, price range constraints are also applied to internal price strategy to protect consumers from receiving too dramatic price change, as shown in below.

$$\pi_{Min} \leq (\pi_{base} + \Delta\pi_t) \leq \pi_{Max} \quad (\forall t \in T) \tag{5.3}$$

The constraints to guarantee the revenue adequacy of the microgrid operators should also be included [82]. The total revenue collected by microgrid operator should be able to cover operation cost and a fair return for resource investment. With IPDSM model implemented, the revenue of microgrid operator should not be less than the value they can collect without IPDSM. Those constraints, as modeled by (5.4), give the incentive for the operator to adopt IPDSM model.

$$\sum_{j\in J}\sum_{t\in T} p_{j,t}^{Load}(\pi_{base}+\Delta\pi_t) \geq \sum_{j\in J}\sum_{t\in T} p_{j,t,base}^{Load}\pi_{base} \tag{5.4}$$

For the internal pricing policy generated by IPDSM model, it is important to ensure the financial equality among different load groups. To achieve this goal, cross-subsidizations [83] among different load groups should be prevented. The payment collected from a given load group should be sufficient to cover the operation cost induced by this group. Those constraints are defined by (5.5).

$$\sum_{t\in T} p_{j,t}^{Load}(\pi_{base}+\Delta\pi_t) \geq \sum_{t\in T} p_{j,t,base}^{Load}\pi_{base} \quad (\forall j \in J) \tag{5.5}$$

Combining the microgrid formulations defined in (3.1) - (3.15) with the IPDSM formulations defined in (5.1) - (5.5), the deterministic IPDSM model for microgrid can be formulated as mixed integer quadratic constrained quadratic programming (MIQCQP) problem. The solution method will be discussed in the following part.

5.3.2 Stochastic IPDSM Model

Considering the stochastic nature of renewable energy generation, there are a significant amount of uncertainties in the microgrid operation scheduling process. The under-estimate of those uncertainties may lead to insufficient system reserve while over-estimation can result in uneconomical operation. Also, because the behavior patterns of human being sometimes are too complex to be modeled perfectly, the estimation of price elasticity for a given load group will also bring randomness into microgrid operation scheduling. Therefore, the stochastic formulation can be helpful here to achieve more robust solution [34, 84].

Taking all these random parameters into consideration, the objective function of stochastic IPDSM model can be formulated into two-stage stochastic programming problem as shown in (3.16) in Chapter 3.

The stochastic objective function can be divided into two parts. The first part is the same as the deterministic formulation while the second part is the recourse cost of resource storage due to a certain operation schedule represented by a mathematical expectation with the consideration of the probability distributions of all the random parameters. Applying all the constraints defined in the deterministic model, the stochastic model can be formulated. Considering the fact that available renewable generations and price elasticity of each load group have continuous probability distributions. Therefore, it is not a trivial task to obtain an analytical solution for the stochastic IPDSM model. The solution technique for this type of stochastic program is discussed in the following section.

5.4 Solution Approach

5.4.1 Deterministic IPDSM Model Solution Method

Aforementioned, the deterministic IPDSM model is formulated as MIQCQP problem. This type of problem can be written in the following form (for notation brevity, x is used to represent the decision variables.).

$$Min\ 0.5x^T Hx + fx \tag{5.6}$$

Subject to

$$x^T Q_j x + q_j x \le r_j \ \ (j \in J) \tag{5.7}$$

$$A_{ineq} x \le b_{ineq} \tag{5.8}$$

$$A_{eq} x = b_{eq} \tag{5.9}$$

From computational complexity point of view, it is desired to have all the Q_j as positive semi-definite matrix in this formulation. If this statement is true, then quadratic constrained problem is a convex programming problem, which can be solved in polynomial time. Otherwise, the problem becomes a NP-Hard problem [52, 85]. There are

multiple choices of commercial off-the-shelf solvers that are able to solve convex quadratic constrained programming problem. However, if the problem is non-convex, then heuristic method can be used as a solving approach.

In the deterministic IPDSM formulation, the quadratic constraints are formed by (5.4) and (5.5). The Q_j in (5.5) is shown by (5.10). It is reasonable to assume that the price elasticity for load group j will always be non-positive [79]. Thus the Q_j in (5.5) is always positive semi-definite. Note that constraint (5.5) actually is a sufficient condition for (5.4). Therefore, it can be concluded that all the quadratic constraints in the deterministic IPDSM model are positive semi-definite. Thus the formulation is convex programming problem, which can be solved by multiple commercially available solvers.

$$Q_j = \begin{bmatrix} 0 & & & \\ & \ddots & & \\ & & 0 & \\ \hline & & -\frac{p_{j,1,base}^{Load}\varepsilon_{j,1}^{Load}}{\pi_{base}} & \\ & & & \ddots \\ & & & -\frac{p_{j,T,base}^{Load}\varepsilon_{j,T}^{Load}}{\pi_{base}} \end{bmatrix} \tag{5.10}$$

5.4.2 Stochastic IPDSM Model Solution Method

As mentioned above, the continuous probability distribution of the random parameters in stochastic formulation would generate infinite number of realizations to completely represent the expectation, which make the problem impractical to solve. To overcome this difficulty, sampling average approximation (SAA) method is applied [34] to solve this problem.

The uncertainty modeling for the renewable generations has been discussed in Chapter 2. The estimation error of price responsive patterns depends on the randomness of end-users' utility and opportunity cost during different operation periods [30-32, 79]. In

this chapter, the price elasticity of different load groups is estimated separately. Customers with similar price responsiveness are categorized into the same load group. Through this approach, the price elasticity estimation can achieve a better accuracy [33, 86]. For each load group, the probability distribution of price elasticity is assumed to follow a uniform distribution.

By implementing Monte Carlo sampling method, N realizations of random vector (composed by all the random parameters) can be generated. Each realization of random vector is a microgrid operation scenario. Considering the Law of Large Number, the stochastic objective function can be re-written as the SAA form. Similarly, constraints that contain random parameters can also be reformulated. It can be observed that the stochastic IPDSM model can be converted to a deterministic MIQCQP problem by applying SAA method and Monte Carlo sampling. Considering the fact that the stochastic price elasticity parameters are non-positive, the Q matrices of quadratic constraints will also be positive semi-definite. Therefore, the stochastic IPDSM model is a convex formulation thus can be solved by commercially available solvers.

5.5 Numerical Study

In this section, a six-bus sample microgrid is presented to illustrate and compare the proposed IPDSM models. Also, the proposed models are implemented to a 30-bus microgrid for scalability study purpose. The models are coded in Matlab and solved by CPLEX 12.5.1[53]. All the experiments are implemented on a computer with AMD X6 CPU@2.70 GHz and 8 GB memory.

5.5.1 System Configuration

The sample microgrid is composed of three fossil-fuel units, one energy storage system, one aggregated wind farm, one aggregated solar station, and loads. The detailed fossil-fuel generator data is scaled from ERCOT operation scheduling, as shown in Table

5-1. The energy storage system data is shown in Table 5-2. The wind and solar power data is obtained from a generation site in Oklahoma. The topology of the microgrid is shown in Figure 3-1.

As mentioned above, the dethe demand side of microgrid is modeled by J different load groups. It should be noted that J should be determined by the characteristics of all microgrid loads, which can be estimated through the techniques discussed in [30-32]. In the sample microgrid, the system demand, which includes industrial, commercial and residential loads, is categorized into three groups based on their price responsive patterns. Load group 1 is assumed to be composed of loads that do not have price sensitivity. Load group 2 is composed of loads that have medium price responsiveness. Load group 3 is composed of loads that have high price sensitivities. Since loads with different responsiveness are addressed separately, a better comprehensive demand side response to the price change can be achieved. Also, the financial equality among different types of consumers with different price response patterns therefore can be protected. The detailed configuration of loads is illustrated by Figure 5-1 and Figure 5-2. It should be noted that the probability distribution of price elasticity is modeled as a uniform distribution within the ± 30% of the deterministic estimation.

Table 5-1 Generator Operation Data

Unit	Max/Min Output (MW)	Ramp Up/Down Rate (MW/h)	Min Up/Down Time (h)
G1	120/15	47/65	4/5
G2	70/15	27.5/35	3/3
G3	40/10	20/42.5	2/3

Table 5-2 Energy Storage System Data

Storage Capacity (MWh)	Max Storage Level	Min Storage Level
100	90%	10%
Max Discharge Rate (MW)	Discharge Efficiency	Initial Storage Level
10	85%	50%
Max Charge Rate (MW)	Charge Efficiency	Final Storage Level
15	85%	50%

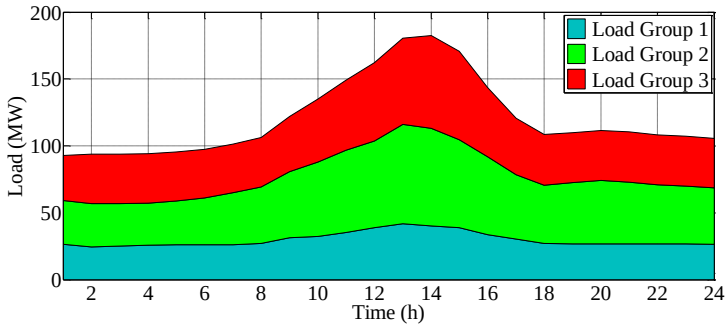

Figure 5-1 Aggregated profiles of each load group

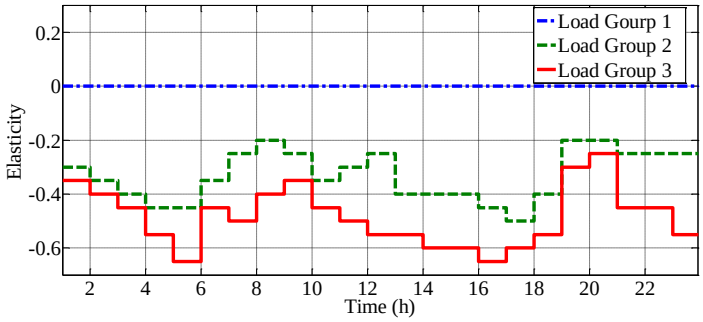

Figure 5-2 Deterministic estimation of load elasticity for each load group

5.5.2 Deterministic IPDSM Model

Initially, the deterministic IPDSM model is implemented to achieve optimal internal price strategy and operation schedule. The solutions are shown in Figure 5-3 to Figure 5-6. It can be observed that fossil units operation schedule under dynamic internal pricing strategy are able to avoid starting up the expensive generator 3. Also, the

operation hours of generator 2 are reduced comparing with the schedule under flat pricing strategy. Figure 5-5 and Figure 5-6 show that the microgrid demand peak is effectively reduced by increasing the price during those hours.

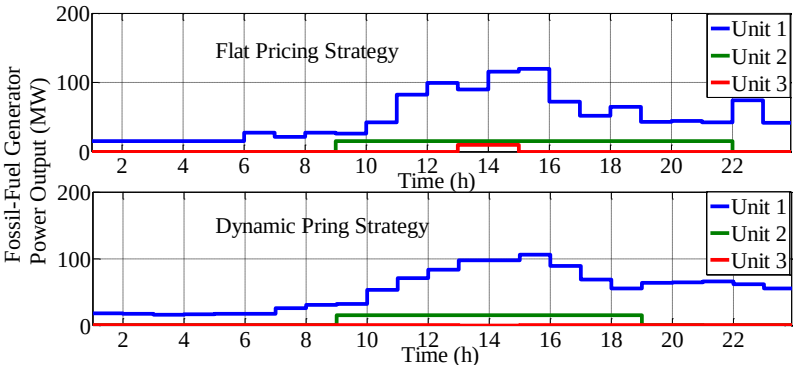

Figure 5-3 Deterministic optimal operation schedule of fossil-fuel units

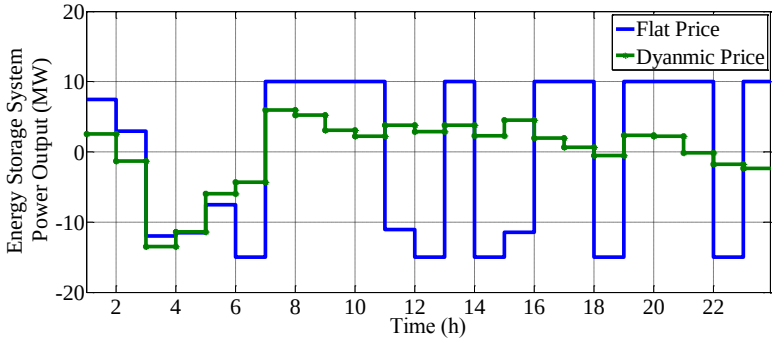

Figure 5-4 Deterministic optimal operation schedule of energy storage system

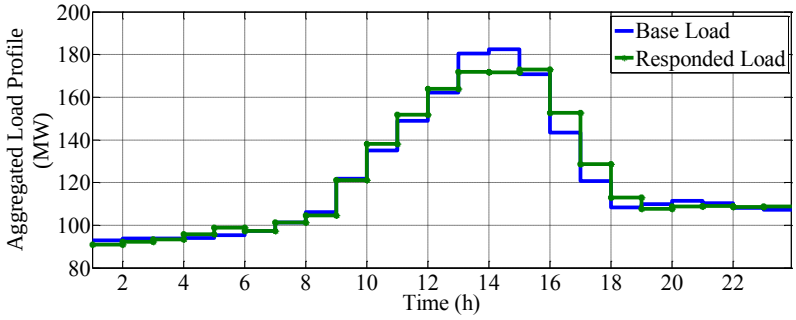

Figure 5-5 Microgrid aggregated load profile under flat and dynamic pricing strategy, deterministic model

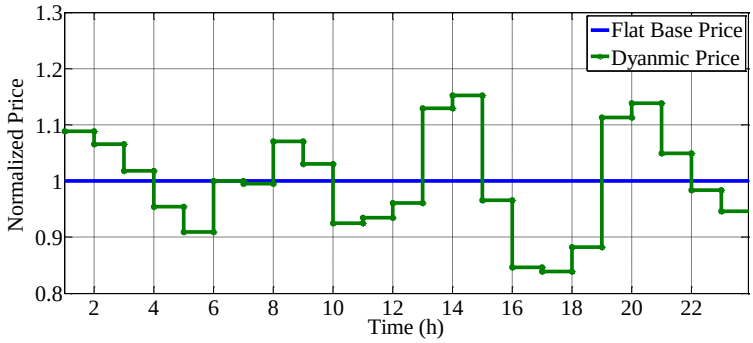

Figure 5-6 Normalized dynamic price policy versus flat base price, deterministic model

Table 5-3 Microgrid Operation Cost for Deterministic IPDSM Model

Pricing Strategy	Flat	Dynamic
Microgrid Operation Cost ($)	36807.3	35572.1
Total Consumption (MWh)	29013.6	29100.9
CPU Time (sec)	0.11	3.85

As depicted in Table 5-3, the total microgrid operation cost under dynamic pricing strategy is reduced while its total load consumption remains the same, comparing with flat pricing strategy. Therefore, it can be concluded that deploying IPDSM model effectively benefits the microgrid operation by optimally reallocating the responsive demands. Another observation is that the total consumption is not reduced significantly. This was expected since the consumption is restrained by constraints that are included to guarantee the generation revenue adequacy and prevent the cross-subsidization among different load groups.

5.5.3 Stochastic IPDSM Model

To address the uncertainties in microgrid operation, operation schedule is solved by the Stochastic IPDSM model with 50 scenarios. The solutions are depicted in Figure 5-7 to Figure 5-10 and Table 5-4.

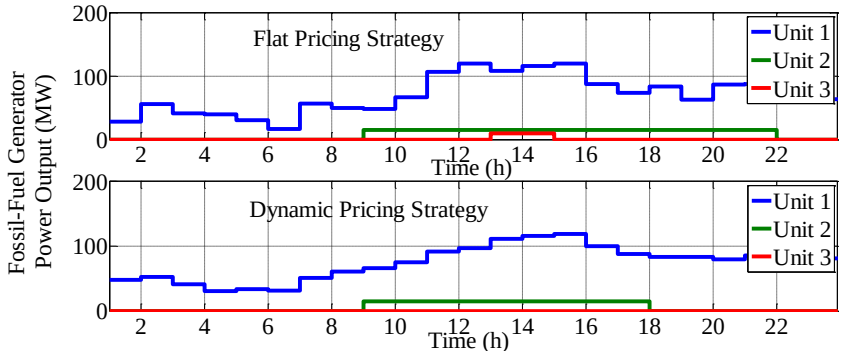

Figure 5-7 Stochastic optimal operation schedule of fossil-fuel units

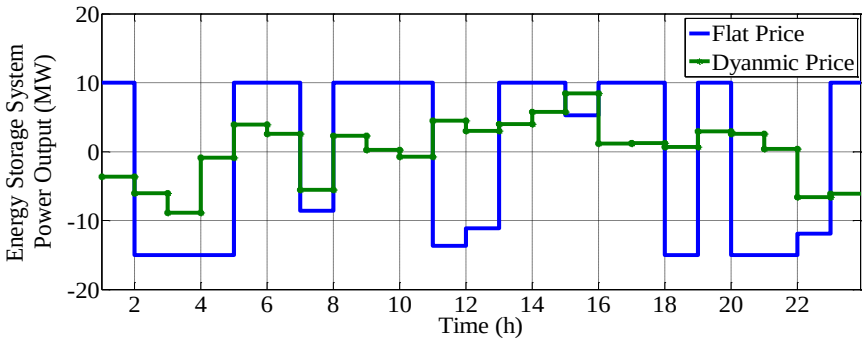

Figure 5-8 Stochastic optimal operation schedule of energy storage system

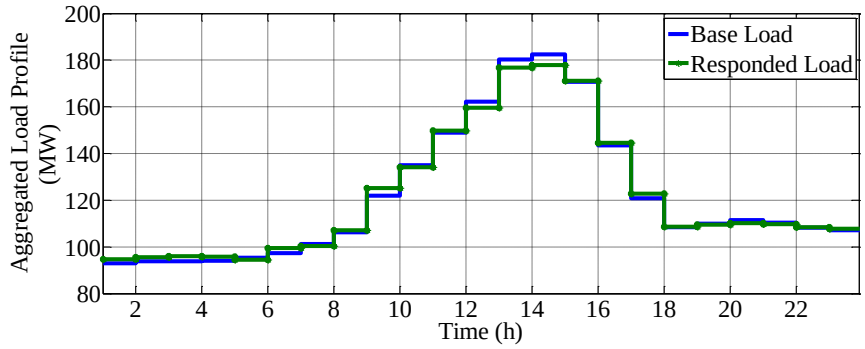

Figure 5-9 Microgrid aggregated load profile under flat and dynamic pricing policy, stochastic model

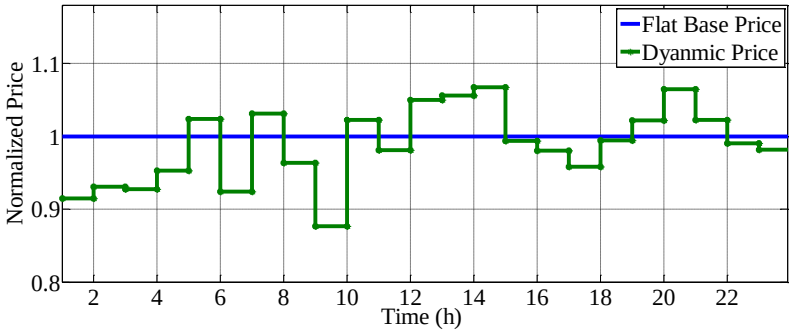

Figure 5-10 Normalized dynamic price policy versus flat base price, stochastic model

Table 5-4 Microgrid Operation Cost for Stochastic IPDSM Model

Pricing Strategy	Flat	Dynamic
Microgrid Operation Cost ($)	47444.7	45924.1
Total Consumption (MWh)	29013.6	29091.3
CPU Time (sec)	0.31	8.62

Comparing Table 5-3 and Table 5-4, it can be observed that the total operation costs of stochastic IPDSM model are higher than deterministic model for both flat and dynamic pricing strategy. This was expected since the optimal value of a convex deterministic optimization is biased upward relative to one of corresponding stochastic optimization, according to Jensen's inequality [34]. The difference between the optimal values of deterministic and stochastic models is the value of perfect information.

To further exploring the stochastic parameters' effects on the optimal solution, sensitivity analysis of renewable energy forecasting standard deviation is conducted. In Figure 5-11, the wind power sensitivity test is performed by changing the normalized standard deviation while keeping other stochastic parameters constant as depicted in system configuration part. Similar tests are also performed for solar power. It can be observed that as the variance of wind and solar power forecasting increasing, the objective total cost is also increasing. In other words, a less deviated stochastic

renewable generation forecasting result will lead to a less costly solution through stochastic IPDSM model. This was expected because a larger variance implies there is a larger probability to have a lower realization of renewable generation with a constant number of scenario samplings. Consequently, the recourse cost will result in a higher-cost operation schedule. It should also be noted the sensitivity of wind power is more significant than solar power. This is because the installed capacity of wind power in the example microgrid is much larger than solar power.

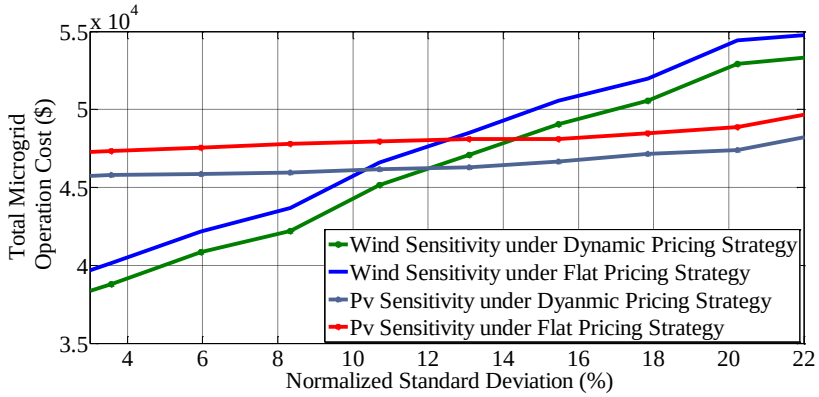

Figure 5-11 Total microgrid operation cost versus normalized standard deviation of renewable generation forecasting error

Figure 5-12 shows sensitivity test for price elasticity estimation error. As the estimation error increasing, the objective total operation cost does not monotonically increase. This is because constraints related to price elasticity (i.e. constraints defined by (5.2), (5.3) and (5.4)) are different from the constraints related renewable generation. We have to apply both upper bound and lower bound to the IPDSM model. Thus the variance level of price responsiveness estimation is neither positively nor negatively correlated to total operation cost.

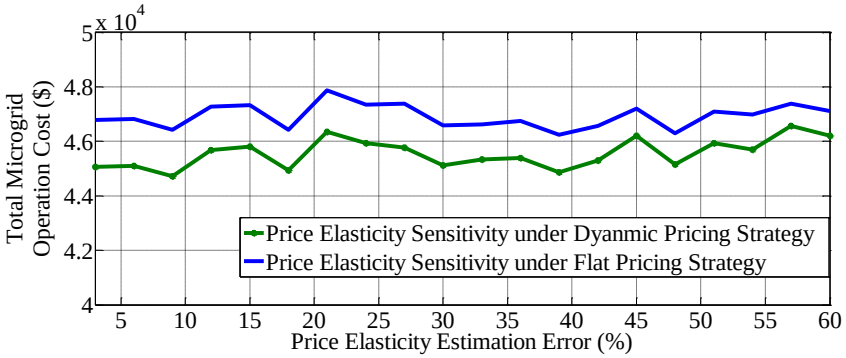

Figure 5-12 Total microgrid operation cost versus estimation error of price elasticity of loads

Figure 5-13 depicts the relationships between the number of scenarios considered in the stochastic model and total microgrid operation cost. If infinite large number of scenarios are considered in the stochastic IPDSM model, SAA formulation would be an unbiased and consistent estimator of original formulation [34]. From Figure 5-13, it can be noted that the total operation cost is converging as the number of scenarios increasing. Another observation from Figure 5-13 is that the objective operation cost is larger if more scenarios are considered. This is because more scenarios imply there would be a higher probability for the operation schedule to be bounded by more rigorous constraints. However it also means the operation schedule is more robust with respect to variations of the stochastic parameters.

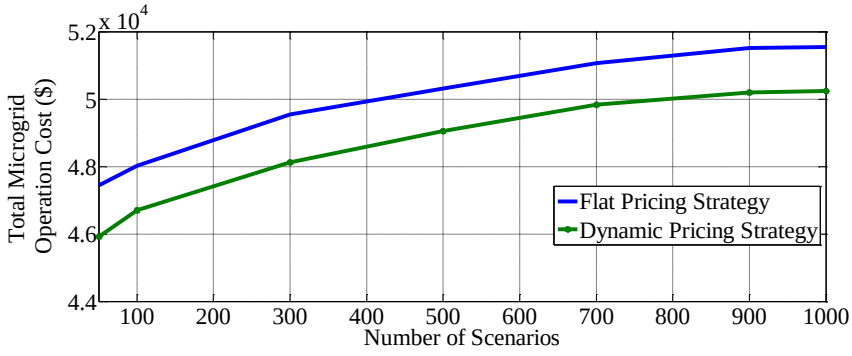

Figure 5-13 Total microgrid operation cost versus number of scenarios

5.5.4 Scalability Test on 30-Bus Microgrid

A 30-bus microgrid modified from IEEE 30 bus test case is used to test the computational burden of proposed IPDSM models on a larger system. There are 18 fossil-fuel generators, one energy storage system, one aggregated wind farm, one aggregated solar station considered in this 30-bus microgrid. Similar to the previous case, the data for the fossil-fuel units is also scaled from ERCOT operation scheduling. The energy storage system data is scaled from a lithium-ion battery system project in China and the wind and solar power data is obtained from a generation site in Oklahoma.

Table 5-5 30-Bus Microgrid Operation Cost for Deterministic IPDSM Model

Pricing Strategy	Flat	Dynamic
Microgrid Operation Cost ($)	216877.7	208535.3
Total Consumption (MWh)	154065.6	154223.5
CPU Time (sec)	0.33	75.65

Table 5-6 30-Bus Microgrid Operation Cost for Stochastic IPDSM Model

Pricing Strategy	Flat	Dynamic
Microgrid Operation Cost ($)	267430.1	256925.8
Total Consumption (MWh)	154065.6	154186.5
CPU Time (sec)	0.58	188.57

Both deterministic and stochastic IPDSM models are implemented on this microgrid system and computational results are reported in Table 5-5 and Table 5-6. In the stochastic model, 50 scenarios are considered in the solving process. Comparing those two tables with Table 5-3 and Table 5-4, it can be noted that solving 30-bus microgrid case takes longer CPU time than solving 6-bus system. This was expected

since the increased number of fossil-fuel generators implies increased number of integer decision variables that indicates the states of fossil-fuel units. Another observation is dynamic pricing strategies for both deterministic and stochastic models take longer times to solve. This is because dynamic pricing formulation is a MIQCQP problem while flat pricing formulation is a mixed integer linear programing (MILP) problem. To sum up, the proposed models can solve the day-ahead resource scheduling problem within an acceptable time considering the typical dimension of microgrid. Therefore, it can be concluded that the proposed IPDSM models are scalable to solve large-scale microgrid resource scheduling problems.

5.6 Summary

This chapter proposes a stochastic resourcing planning model to optimize microgrid operation. By reallocating the price responsive demands through a dynamic internal price signal, the operation cost of microgrid can be reduced. The stochastic characteristics of renewable generations forecasting and demand price responsiveness estimation are addressed in the proposed model. Also, the incentives for implementing this IPDSM model for both microgrid system operator and end-user customers are included in the constraints. Case study results illustrate that stochastic IPDSM model can reduces the microgrid operation cost while provides a robust operation schedule. Further analysis for the characteristics of stochastic solution is also discussed. In this chapter, the IPDSM model is formulated via a centralized approach since multiple constraints, such as resource revenue adequacy and financial equality, are considered in a globalized manner. Considering the further developments of smart grid technologies and increased privacy concerns on the demand side, a future development of this work can be implementing the proposed IPDSM model via a decentralized approach.

Chapter 6

Medium-term Operation of Microgrid in a Deregulated Power Market

6.1 Literature Review

Under a deregulated market environment, grid-connected microgrids can participate in multiple markets with different time scales [87-92], such as forward market, day-ahead market and real-time market, to procure electricity for their loads. The procurements settled by different markets may involve different levels of cost uncertainties and risks [93]. For example, a microgrid can sign a bilateral forward contract to reduce the risk associated with volatility of future electricity purchase price. However a lower risk level contract typically comes with a higher procurement cost which can be considered as a risk premium [94]. On the other hand, settlements on day-ahead market or real-time market may lead to a lower average cost however they also result in a higher level of volatility on the procurement expense, which is undesired. Therefore, an microgrid has to comprise its procurement portfolio by determining its involvements in different types of market. To balance this potential trade off, a medium-term energy procurement portfolio problem becomes critical to microgrids to minimize their costs and manage their risks.

Though the medium-term energy procurement models for electricity retailers have been addressed in numbers of research papers, limited efforts have been devoted to developing a medium-term decision making model for microgrids. Liu *et al.* [94] proposed an optimal energy purchase allocation and demand bidding scheme for an electric energy service provider. Woo *et al.* [95] presented a risk-constrained procurement model for a distribution company. The risk level was measured by value-at-risk (VaR) in [3]. Xu *et al.* [96] proposed a medium-term procurement portfolio optimization model for a load serving entity (LSE) which used semi-variance of spot

market transactions as risk term. Kettunen *et al.* [97] established a multi-stage stochastic model to minimize the procurement cost subject to a set of risk constraints. Woo *et al.* [98] derived a set of Pareto-optimal solutions for the purchase allocation of a distribution company. Carrion *et al.* [99] presented a risk-constrained stochastic model for procurement decision and price determination of a electricity retailer. The pool price was characterized using time-series model in this paper. Carrion *et al.* [100] also proposed a bi-level programming approach to solve the medium-term decision making problem faced by a retailer. Those reviewed literatures have provided effective studies for the medium-term energy procurement model for retailers or distribution companies. However, the day-ahead market settlements and real-time market settlements have not been distinguished when modeling the pool price in most cases. As an important tool designed for hedging the volatility in real-time market price, the characteristics of day-ahead market settlement price play a critical role in determining the medium-term energy procurement portfolio for grid-connected microgrids.

Considering the unique operating characteristics of microgrids, it is possible to incorporate the DSM into the medium-term operation decision making model. Although the DSM, or demand response (DR), for microgrids have been studied in multiple papers as mentioned in Chapter 5, their capability for hedging the variance on the real-time settlement price has rare been considered in the medium-term operation model. As the operators of those microgrid facilities have better knowledge of the economic responsiveness of each load sector, microgrids can utilize DSM to manage the volatility risks of their energy procurement cost.

Taking all above into consideration, this chapter proposes a medium-term operation model for a grid-connected microgrid. Multiple market settlements, which include forward contract settlement, day-ahead market settlement, and real-time market

settlement, have been considered in this model. Also, the DSM of microgrid is implemented in this model as a hedging tool to reduce the risks. The model is formulated as a stochastic quadratic programming (SQP) problem which can be efficiently solved by commercial solvers. The risk term is measured by mean-variance risk model in the proposed formulation. The uncertainties in the formulation are characterized by stochastic day-ahead and real-time price models which are generated from historical ERCOT data. It should be mentioned that the load considered in this chapter are the net effective load from the bulk power system point of view. In other words, the load considered is the net load which has been subtracted by the microgrid distributed generations. For simplification purpose, the scheduling of the microgrid generation has not been considered in this chapter. The details of scheduling operation for microgrid can be referred to Chapter 3 in this dissertation.

6.2 Medium-term Operation Framework

As aiming to establish a medium-term operation framework for a microgrid, multiple operation decisions, which include energy procurements and DSM, should be made within a medium time span. Without loss of generality, a time span of one week is considered in this chapter. The decisions made by the microgrid can be classified into two categories: medium-term decisions and day-ahead decisions, as shown in Fig. 1.

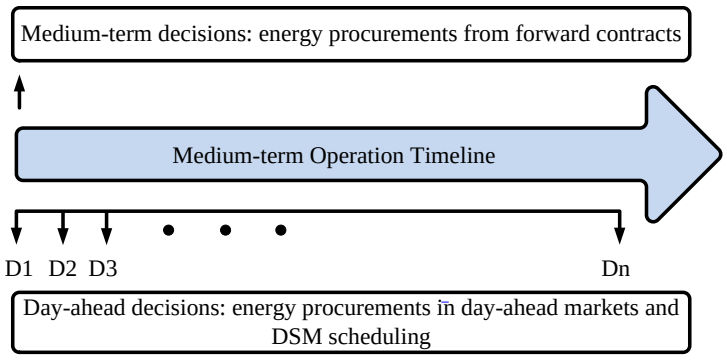

Figure 6-1 Medium-term operation timeline for a microgrid

In the proposed medium-term operation framework, a microgrid is assumed to make multiple decisions at different time points. The available information for different time points also vary therefore decisions would be made under different level of uncertainties. In this paper, the uncertainties of the information are characterized by stochastic price models, which will be discussed in details in the following part of this chapter.

6.2.1 Medium-term Decisions

The microgrid is assumed to be able to participate in forward market to obtain energy for its loads. Therefore the medium-term operation decisions would be made to determine the amount of energy purchased through forward contracts. Three different types of forward contracts are considered: peak weekday (PWD), peak weekend (PWE), and off peak (OP). Since those medium-term decisions are made at the beginning of the time span, the information available at that time point would be imperfect. Therefore the realizations of day-ahead settlement price and real-time settlement price during this time span are treated as random parameters while the settlement prices and specifications for those forward contracts are assumed as known in this model. The microgrid would select the optimal offers from the forward markets for different contract types and make the decisions for the amount of procurement. In this chapter, the base load of microgrid is assumed as perfect information for medium-term decision making.

6.2.2 Day-ahead Decisions

After signing the procurements contracts in the forward markets, the microgrid needs to participate in the day-ahead market and determine the DSM schedule prior to every operation day. Figure 6-2 shows the timeline for making day-head decisions. It should be noted that the time points shown in Figure 6-2 are adopted from current

ERCOT market protocol [101], however the proposed day-ahead decision making model can be modified and adapt to other market protocols.

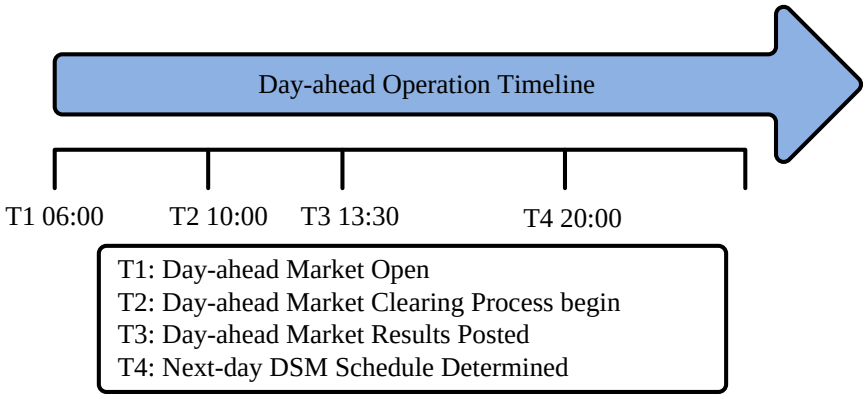

Figure 6-2 Day-ahead operation timeline for microgrid

As shown in Figure 6-2, the day-ahead market is assumed to be open at 06:00 AM and close at 10:00 AM. The microgrid should submit its bid to purchase through the qualified scheduling entity (QSE) during this period. The bid should be determined based on procurements on the forward market, the updated forecasting result for the next-day real-time settlement price, and the anticipation of the next-day load baseline. After 10:00 AM the independent system operator (ISO) would run the day-ahead market clearing engine and post the market clearing results at 13:30 PM [101]. Based on this result, the microgrid would know the quantity of energy that has been purchased in the day-ahead market and determine its DSM schedule for the next operation day. After all those decisions made, the difference between actual demand realization and its procurement amount would be compensated by real-time market and settled by corresponding prices.

6.2.3 Demand Side Management

For microgrids, curtailments of non-critical loads and rescheduling some of their production processes are typically feasible [102, 103]. In this chapter, the microgrid is assumed to have a clear knowledge of the long-term economic impacts of the curtailment

or rescheduling of its loads. Consequently, the financial impacts of those interruptible loads can implicitly define the responsiveness of those loads to the electricity price. In the proposed model, the loads of this microgrid are categorized into different load classes based on their price responsiveness. Through this approach, the responsive pattern of each load class can be addressed separately considering the fact that the monetary value of interruptible load for each load class may change along with time thus their price responsiveness would be time-variant parameters.

Considering the characteristics of microgrid, it can be difficult to achieve curtailment of non-critical loads and rescheduling of production processes in a real-time manner [104]. Therefore, in the proposed model, the schedule of DSM for the microgrid is determined prior to the next-operation day. It should also be noted that the responsiveness of each load class is determined by the effective settlement price. At the time point for making DSM decisions, the effective settlement price is determined by the procurements in forward and day-ahead market, the settlement prices in forward and day-ahead market, and the forecasting result of next-day real-time settlement price. Combining this effective settlement price with price elasticity (i.e. price responsiveness) of each load group, final DSM schedule can then be determined

6.2.4 Risk Management

Considering that the realizations of day-ahead settlement price and real-time settlement price are random parameters for medium-term operation model, microgrid may experience extreme volatility for its total energy purchase cost. To explicitly quantify this risk term for energy procurement portfolio, mean-variance risk model [105] is implemented in this chapter. As one of the fundamental theories for modern portfolio theory [106], mean-variance risk model is a quantitative tool to achieve trade-off between expected cost (or return) and risk. Based on this principle, multiple operation options,

which include purchase via forward contracts, purchase in day-ahead market, purchase in real-time market and DSM, form a decision portfolio and can be optimized to minimize the total energy procurement cost and the corresponding volatility risk. The mathematic formulation of this portfolio optimization problem is discussed in details in the following sections.

6.3 Price Modeling and Uncertainty Characterization

In order to optimize the medium-term energy procurement portfolio for the microgrid, the price uncertainties in the day-ahead and real-time markets need to be considered. The study of price modeling has been reviewed in [107]. The stochastic price can be determined by normal distribution [108, 109]. However, taking the price spike scenarios in deregulated market environments into consideration, the price uncertainty sometimes may follow the lognormal distribution [110]. In this paper, two stochastic price models are formulated based on 2011 ERCOT market price data [111] to characterize the randomness of day-ahead and real-time settlement prices, respectively. For comparison purpose, both summer and winter cases are considered in this paper to demonstrate different price scenarios and their impacts on the energy procurement portfolio.

In the proposed formulation, the decisions are made on an hourly basis. Considering that ERCOT publishes the real-time settlement price for every 15-minute interval, the real-time market in this paper is evaluated by a load-weighted average settlement price. Since the forward markets are separated into three different time period, the day-ahead and real-time prices are also analyzed separately for PWD, PWE, and OP. In the proposed model, PWD is defined as hours ending in 07:00 AM to 10:00 PM for weekday excluding NERC holidays. PWE are hours ending in 07:00 AM to 10:00 PM for weekend and NERC holidays. OP is the rest hours [101].

Table 6-1 Characteristics of 2011 ERCOT North Load Zone Price Data

	Summer			Winter		
Mean ($/MWh)	PWD	PWE	OP	PWD	PWE	OP
Day-ahead	133.82	75.39	27.89	43.64	31.69	32.07
Real time	116.87	55.87	28.21	45.92	27.25	37.79
Variance ($/MWh)^2	PWD	PWE	OP	PWD	PWE	OP
Day-ahead	114427	19271	32	5587	72	2329
Real time	137411	7943	294	26636	162	25928

Table 6-1 illustrates the mean and variance of day-ahead and real-time market prices in both summer and winter cases. It can be observed that the day-ahead settlement prices are higher than the real-time in most cases. Meanwhile, the variances of the day-ahead settlement prices are greater than the real-time one. This is expected since the purpose of establishing day-head market is to hedge the volatility risks in the real-time market. The mean price difference can be treated as the mean risk premium the market would like to pay for this hedge.

Table 6-2 Probability Distributions of Settlement Price for Specific Time

	Day-ahead Summer		Real-time Summer		Day-ahead Winter		Real-time Winter	
Time	WD	WE	WD	WE	WD	WE	WD	WE
0:00	N	N	LN	LN	LN	N	N	LN
1:00	N	N	N	N	LN	N	N	N
2:00	N	N	N	N	LN	N	N	N
3:00	N	N	N	N	LN	N	LN	N
4:00	N	N	N	N	LN	N	LN	N
5:00	N	N	N	N	LN	N	LN	N
6:00	N	N	N	N	LN	LN	LN	LN
7:00	N	N	N	N	LN	N	LN	N
8:00	N	N	N	N	LN	N	LN	LN
9:00	N	N	LN	LN	LN	LN	LN	LN
10:00	N	LN	N	N	LN	N	LN	LN
11:00	N	N	N	N	LN	N	LN	N
12:00	N	N	LN	N	LN	N	LN	LN
13:00	LN	LN	LN	LN	LN	N	LN	N
14:00	LN	LN	LN	LN	LN	N	LN	N
15:00	LN	LN	LN	LN	LN	N	LN	N

Table 6-2—*Continued*

16:00	LN	LN	LN	LN	LN	N	LN	N
17:00	LN	LN	LN	LN	LN	N	LN	N
18:00	LN	LN	LN	LN	LN	LN	LN	LN
19:00	LN	LN	LN	LN	LN	N	LN	N
20:00	LN	LN	N	N	LN	LN	LN	LN
21:00	LN	LN	LN	N	LN	N	LN	N
22:00	N	N	LN	LN	LN	N	LN	LN
23:00	N	N	LN	LN	LN	N	N	N

N is Normal Distribution and LN is Lognormal Distribution

Considering these different characteristics, the realization of day-ahead and real-time settlement prices during these time periods should be modeled separately. In this paper, the price distributions for specific time period are evaluated on an hourly basis by ARENA [112] as reported in Table 6-2. From the analysis results, it can be observed that the price distributions for different time period fit with either normal distribution or lognormal distribution according to the results of Kolmogorov-Smirnov test. For the same hour of a day in different seasons, the price distribution may follow different types of probability distribution. For example, Figure 6-3(a) shows the settlement price distribution in day-ahead market PWE in summer at the period ending by 9:00 AM. The characteristic of this time period price model can be represented by normal distribution with 31.7 and 2.41 of mean and standard deviation, respectively. Meanwhile, as shown in Figure 6-3(b), the PWE settlement price distribution model in day-ahead market at the same hour of a day in winter is comparatively distinguished to the summer price by fitting with a lognormal distribution with mean and variance of 34.7 and 59.92, respectively.

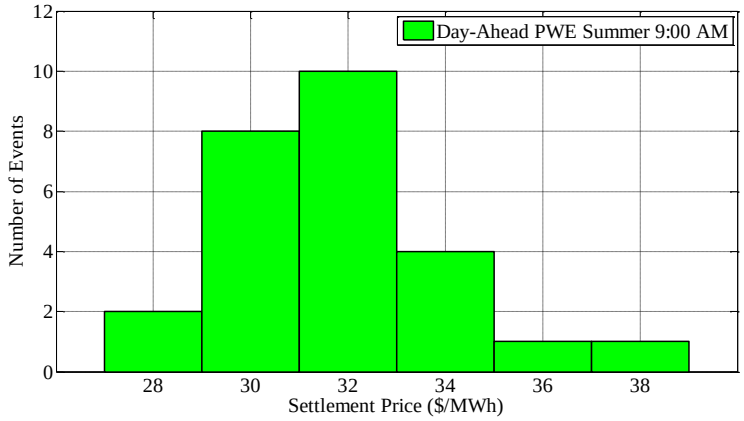

(a)

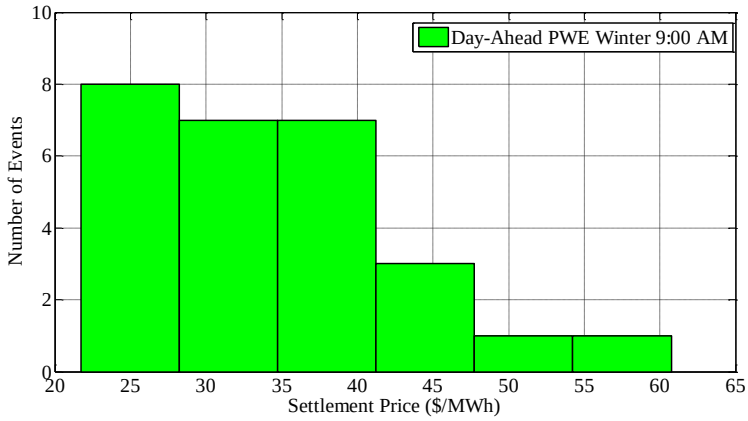

(b)

Figure 6-3 Price distribution for day-ahead PWE at 9:00 AM (a) Summer (b) Winter

6.4 Mathematical Formulation

Aforementioned, the proposed medium-term operation model for microgrid is formulated as a SQP problem, as shown in the following.

$$\begin{aligned} Min \sum_{t\in T_{PWD}} p^{F}_{PWD,t}\pi^{F}_{PWD} + \sum_{t\in T_{PWE}} p^{F}_{PWE,t}\pi^{F}_{PWE} + \sum_{t\in T_{OP}} p^{F}_{OP,t}\pi^{F}_{OP} \\ + \sum_{s\in S}\sum_{t\in T} prob_s \left(p^{DA}_{t,s}\pi^{DA}_{t,s} + p^{RT}_{t,s}\pi^{RT}_{t,s} \right) + \beta \cdot Var \end{aligned} \tag{6.1}$$

Subject to:

Energy volume constraints for forward contracts

$$E^F_{PWD,\min} \le \sum_{t\in T_{PWD}} p^F_{PWD,t} \le E^F_{PWD,\max} \tag{6.2}$$

$$E^F_{PWE,\min} \le \sum_{t\in T_{PWE}} p^F_{PWE,t} \le E^F_{PWE,\max} \tag{6.3}$$

$$E^F_{OP,\min} \le \sum_{t\in T_{OP}} p^F_{OP,t} \le E^F_{OP,\max} \tag{6.4}$$

Energy consumption constraints for forward contracts in each operation period

$$p^F_{PWD,\min} \le p^F_{PWD,t} \le p^F_{PWD,\max} \quad \left(\forall t \in T_{PWD}\right) \tag{6.5}$$

$$p^F_{PWE,\min} \le p^F_{PWE,t} \le p^F_{PWE,\max} \quad \left(\forall t \in T_{PWE}\right) \tag{6.6}$$

$$p^F_{OP,\min} \le p^F_{OP,t} \le p^F_{OP,\max} \quad \left(\forall t \in T_{OP}\right) \tag{6.7}$$

Mean-variance constraints

$$Var = Var\left\{\sum_{s\in S}\sum_{t\in T} prob_s\left(p^{DA}_{t,s}\pi^{DA}_{t,s} + p^{RT}_{t,s}\pi^{RT}_{t,s}\right)\right\} \tag{6.8}$$

Power balance constraints

$$p^F_{PWD,t} + p^{DA}_{t,s} + p^{RT}_{t,s} = \sum_{i\in I} p^{Loadi}_{t,s} \quad \left(\forall t \in T_{PWD}, i \in I, s \in S\right) \tag{6.9}$$

$$p^F_{PWE,t} + p^{DA}_{t,s} + p^{RT}_{t,s} = \sum_{i\in I} p^{Loadi}_{t,s} \quad \left(\forall t \in T_{PWE}, i \in I, s \in S\right) \tag{6.10}$$

$$p^F_{OP,t} + p^{DA}_{t,s} + p^{RT}_{t,s} = \sum_{i\in I} p^{Loadi}_{t,s} \quad \left(\forall t \in T_{OP}, i \in I, s \in S\right) \tag{6.11}$$

DSM constraints

$$\left(p^{Loadi}_{t,s} - p^{Loadi}_{t,base}\right)/p^{Loadi}_{t,base} = \varepsilon^{Loadi}_t\left(\pi^{Eff}_{t,s} - \pi^{Loadi}_{base}\right)/\ \pi^{Loadi}_{base} \quad \left(\forall t \in T, i \in I\right) \tag{6.12}$$

$$\pi^{Eff}_{t,s} = \frac{p^F_{PWD,t}\pi^F_{PWD} + p^{DA}_{t,s}\pi^{DA}_{t,s} + \left(\sum_{i\in I} p^{Loadi}_{t,base} - p^F_{PWD,t} - p^{DA}_{t,s}\right)}{\sum_{i\in I} p^{Loadi}_{t,base}} \ \left(\forall t \in T_{PWD}, s \in S\right) \tag{6.13}$$

$$\pi_{t,s}^{Eff} = \frac{p_{PWE,t}^{F}\pi_{PWE}^{F} + p_{t,s}^{DA}\pi_{t,s}^{DA} + \left(\sum_{i\in I} p_{t,base}^{Loadi} - p_{PWE,t}^{F} - p_{t,s}^{DA}\right)}{\sum_{i\in I} p_{t,base}^{Loadi}} \quad \left(\forall t \in T_{PWE}, s \in S\right) \tag{6.14}$$

$$\pi_{t,s}^{Eff} = \frac{p_{OP,t}^{F}\pi_{OP}^{F} + p_{t,s}^{DA}\pi_{t,s}^{DA} + \left(\sum_{i\in I} p_{t,base}^{Loadi} - p_{OP,t}^{F} - p_{t,s}^{DA}\right)}{\sum_{i\in I} p_{t,base}^{Loadi}} \quad \left(\forall t \in T_{OP}, s \in S\right) \tag{6.15}$$

$$p_{t,\min}^{Loadi} \le p_{t,s}^{Loadi} \le p_{t,\max}^{Loadi} \quad \left(\forall t \in T, s \in S, i \in I\right) \tag{6.16}$$

6.4.1 Objective Function

The objective function (6.1) in the proposed formulation contains two parts: the total energy procurement cost and quantified risk term. The risk coefficient is used to describe the tradeoff between the procurement cost and risk. The value of β represents the level of risk aversion for the microgrid. In other words, the larger β is, the more conservative procurement portfolio the microgrid would choose. Correspondingly, the total energy procurement cost would be higher. Depending on the risk aversion level of the microgrid, a proper value of β should be chosen and implemented in the proposed model. The details on how to determine this β are beyond the scope of this paper, however there are numbers of economic papers have conducted effective research on this topic [113-115].

6.4.2 Constraints for Forward Contracts

In this paper, the forward contracts are defined on different time period: PWD, PWE, OP. The upper and lower energy volume bounds for forward contracts of different time periods are defined by (6.2)-(6.4), respectively. Meanwhile, the energy consumption bounds for each operation periods are defined by (6.5)-(6.7), respectively.

6.4.3 Risk Measurement Constraints

As mentioned above, the risk term is quantified by mean-variance model. In this paper, the procurement volatility risk comes for the uncertainties in the day-ahead market and real-time market. To calculate this value, the covariance matrix among those prices in both market need to be calculated. Based on this covariance matrix, the mean-variance of total procurement cost can be obtained as shown in the following.

$$\begin{aligned} & Var\left\{\sum_{s\in S}\sum_{t\in T} prob_s\left(p_{t,s}^{DA}\pi_{t,s}^{DA}+p_{t,s}^{RT}\pi_{t,s}^{RT}\right)\right\}= \\ & \left(prob_s\right)^2\left\{\sum_{s\in S}\sum_{t\in T}\left(\left(p_{t,s}^{DA}\right)^2 Var\left(\pi_t^{DA}\right)+\left(p_{t,s}^{RT}\right)^2 Var\left(\pi_t^{RT}\right)\right)\right\} \\ & +\left(prob_s\right)^2\left\{\sum_{1\le i<j\le TN} p_i^{DA}p_j^{DA}Cov\left(\pi_{t_i}^{DA},\pi_{t_j}^{DA}\right)\right\} \\ & +\left(prob_s\right)^2\left\{\sum_{1\le i<j\le TN} p_i^{RT}p_j^{RT}Cov\left(\pi_{t_i}^{RT},\pi_{t_j}^{RT}\right)\right\} \\ & +\left(prob_s\right)^2\left\{\sum_{i=1}^{TN}\sum_{j=1}^{TN} p_i^{DA}p_j^{RT}Cov\left(\pi_{t_i}^{DA},\pi_{t_j}^{RT}\right)\right\} \end{aligned} \tag{6.17}$$

It can be observed from (6.17) that the variance is composed of four parts: the self-variance of price in both markets, covariance between different time period in day-ahead market, covariance between different time period in real-time market and covariance between two markets.

6.4.4 Power Balance Constraints

The power balance constraints are implemented by (6.9)-(6.11). The loads in chapter are assumed as net loads from the bulk power system point of view, which the total microgrid loads minus the internal generation behind the point of common coupling. It should be noted that the energy procurement settled in real-time market would be determined by the purchases made in forward and day-ahead market and the actual realization of total demand which is determined by the DSM.

6.4.5 DSM Constraints

In this paper, the price responsiveness of each load group is synthesized from the long-term economic impact of the corresponding interruption and represented by price elasticity, as shown in (6.12). Each load group would response to the effective prices which are defined by (6.13)-(6.15). The upper and lower bounds of the demand response are defined by (6.16).

Combining all those constraints, the medium-term operation model for microgrid is formulated as a SQP problem. By applying Monte Carlo simulation method [34], the SQP problem can be converted as deterministic quadratic programming, which can be efficiently solved by commercial available solvers.

6.5 Numerical Study

The proposed medium-term operation model is applied to an assumed microgrid based on ERCOT electricity market. Both summer and winter cases are studied to illustrate its performance for different price scenarios. The formulation is coded in Matlab and solved by CPLEX 12.5.1 [53]. All the models are implemented on a computer with AMD X6 CPU@2.70 GHz and 8 GB memory.

6.5.1 Case Configuration

Without loss of generality, the microgrid is assumed to have three load classes based on long-term financial impacts of the interruption of their services. Load class 1 is assumed to be critical loads which cannot be interrupted so that they do not have price responsiveness. Load class 2 is composed of loads that have medium financial interruption impact therefore they have medium price elasticity. Load class 3 has relative low financial impact for interruption so that they have low price elasticity. A weekly load profile for this microgrid is illustrated in Figure 6-4 and the corresponding price responsiveness is shown in Table 6-3.

Table 6-3 Price Elasticity of Each Load Class

Load Class	Peak Weekday	Peak Weekend	Off Peak
1	0	0	0
2	-0.1	-0.05	-0.025
3	-0.2	-0.1	-0.05

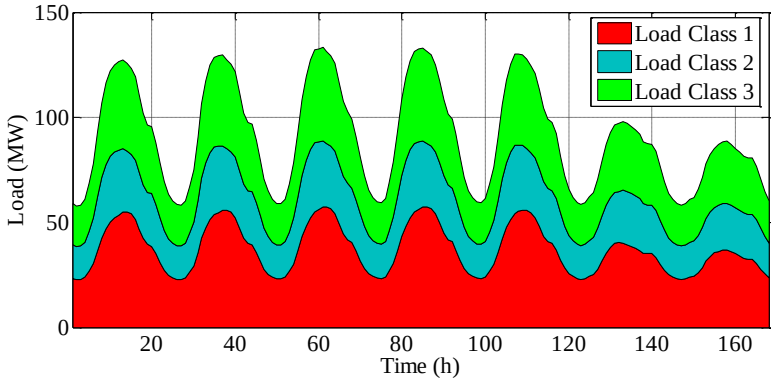

Figure 6-4 Weekly load profile for each load group

In this paper, the microgrid is assumed as a price taker, i.e. it has no influence on the final realization of market prices. At the beginning of the medium-term decision making time frame, the microgrid operator would compare the options in the forward market and choose the best available. The detailed information of the forward contracts is reported by Table 6-4 and Table 6-5.

Table 6-4 Energy Consumption Bounds for Forward Contracts

	Energy Consumption Upper Bounds (MWh)	Energy Consumption Lower Bounds (MWh)
Peak Weekday	5000	1500
Peak Weekend	2000	500
Off Peak	2000	500

Table 6-5 Weekly Forward Contract Settlement Price for Summer and Winter Case

	Summer Week Contracts ($/MWh)	Winter Week Contracts ($/MWh)

Table 6-5—*Continued*

Peak Weekday	137.41	60.33
Peak Weekend	83.23	53.75
Off Peak	37.02	35.48

To compare and illustrate the medium-term operation model in different price scenarios, summer and winter of year 2011 data are applied to generate the stochastic price model in the case study. The prices of the forward contracts are modified from the historical settlement data for ERCOT north load zone in 2011[111].

6.5.2 Simulation Results Analysis

The total procurement cost and volatility risk (i.e. the variance of the total procurement cost) results of summer and winter week for the microgrid are reported in Figure 6-5 and Figure 6-6. It can be observed that the procurement cost increases as long as the risk coefficient increases. In contrast with that, the volatility risk decreases while the risk coefficient increases for both cases. This is because when the risk coefficient increases, the stake-holder of microgrid is more risk-averse. Consequently, in the trade-off between expected cost and risk, the microgrid operator would rather reduce the risk at the cost increasing the expected procurement cost. As a result, the procurement cost decreases while the volatility risk increases.

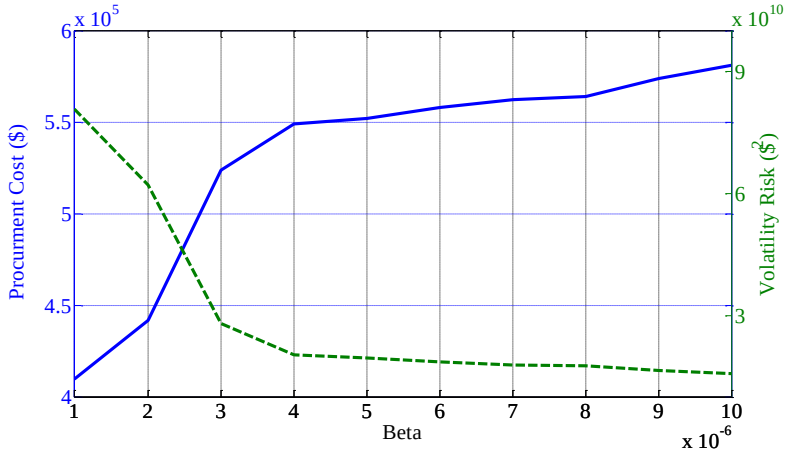

Figure 6-5 Energy procurement cost versus volatility risk in summer for the microgrid

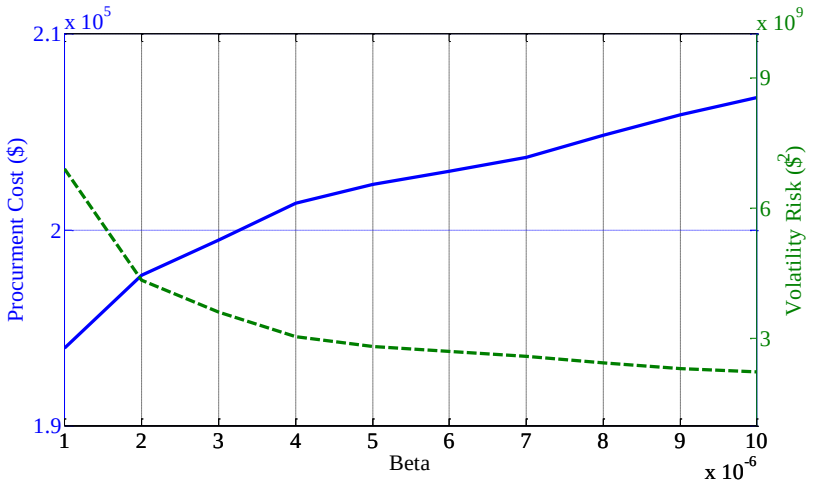

Figure 6-6 Energy procurement cost versus volatility risk in winter for the microgrid

To further explore the impact of risk coefficient, Figure 6-7 is presented to illustrate the difference in the procurement portfolio for different risk preference. The blue column represents a risk-neutral microgrid (i.e. its risk coefficient beta equals to 0) while the red column represents a risk-averse one (i.e. its risk coefficient beta equals to 1). It can be observed that in the procurement portfolio of the risk-neutral microgrid, the percentages of energy procured via forward contracts, via day-ahead market and via real-time market are increasing monotonically. This is because the average settlement prices from those options are decreasing monotonically, as shown in Table VI. Compared with that, the procurement portfolio of the risk-averse microgrid indicates that the percentages of energy purchased via forward contracts, via day-ahead market and via real-time market are decreasing monotonically. This is because the volatility risks associated with those options are increasing monotonically. Due to the risk coefficient beta the risk measurement part carries a large weight in the decision making objective. Consequently the microgrid would prefer the less risky options (i.e. the procurement options with less variance for the price distribution) even though the average settlement prices for those options might be higher.

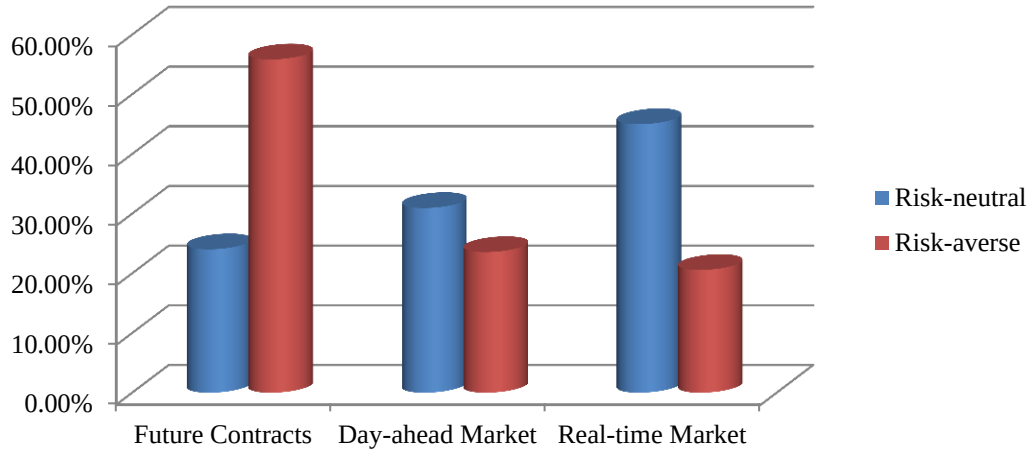

Figure 6-7 Energy procurement portfolio comparison (risk-neutral versus risk-averse)

Table VI shows weighted average settlement prices in different markets for both cases (based on the portfolio solution with risk coefficient beta equals to 1). As mentioned in the section III, the average settlement prices in forward market are the highest and those in real-time market are the lowest. The price differences can be treated as the risk premium [116] which microgrid is willing to pay to reduce the volatility risk of its energy procurement cost. However, it is worth mentioning that the real-time market might be the highest under certain severe weather situation. However, this is considered as outlier case and the procurement decisions are supposed to be made based on medium-term statistical forecasting.

Table 6-6 Weighted Average Settlement Price ($/MWh)

Average Settlement Price	Forward Contracts	Day-ahead Market	Real-Time Market
Summer Case	91.73	82.51	72.69
Winter Case	49.87	40.37	36.41

Figure 6-8 demonstrates the load shifting and peak shaving capability by applying DSM in the day-ahead operation. From the results reported by Table 6-7, it can

be observed that the industry customer can achieve a lower average energy procurement cost by implementing DSM. This can be explained that as the microgrid operator rearranges its next-day operation schedule based on the real-time settlement price forecasting, its consumption during the peak-price hours would be reduced and shifted to lower-price hours. Consequently, the average procurement cost would be reduced. Another observation can be made from Table 6-7 that the consumption reduction in the summer case is more effective than winter case. This is because the average price in summer is higher than winter. Therefore, based on the same price responsiveness, the microgrid should achieve more consumption reduction in the summer scenario as the corresponding incentive is larger.

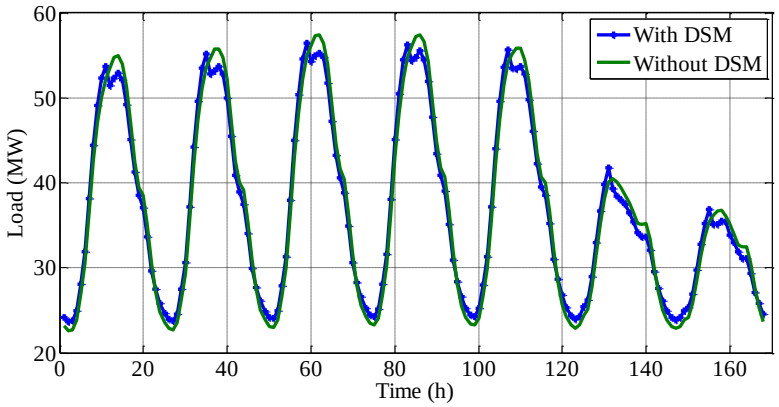

Figure 6-8 Weekly load profile with and without DSM (Summer Case)

Table 6-7 Total Procurement and Consumption with and without DSM

		With DSM	Without DSM
Summer Week	Total Procurement Cost ($)	545837.47	588890.18
	Total Consumption (MWh)	6241.21	6412.83
	Average Price ($/MWh)	87.46	91.83
Winter Week	Total Procurement Cost ($)	284262.11	291527.25

Table 6-7—*Continued*

Total Consumption (MWh)	6377.88	6412.83
Average Price ($/MWh)	44.57	45.46

6.6 Summary

In this chapter, a medium-term operation model is proposed to for microgrid to optimize its operation portfolio. The purchase allocation problem in forward market, day-ahead market and real-time market and demand side management (DSM) are considered to minimize procurement cost and volatility risk faced by the microgrid. The uncertainties in this process are characterized by stochastic price models generated from historical ERCOT data. Then proposed model is formulated and solved by stochastic quadratic programming approach. The case study results illustrate that the proposed medium-term operation model can help the microgrid achieve an optimal procurement portfolio while restraining the volatility risk. Also, implementing DSM help the microgrid reduce the total consumption and achieve lower average price, thus reduce the total procurement cost.

Chapter 7

Conclusions and Future Work

With its technological and regulatory innovation of scale and structure, microgrids have been developed all over the world as a mean to address the high penetration level of renewable generation, reduce the greenhouse gas emission, and provide economical solutions for the currently non-electrified area. The operation of microgrid requires resource planning for those fossil-fuel based generators, energy storage systems, and demand resources if demand side management is implemented. Due to the stochastic nature of renewable energy resources, load behaviors, and market prices, enormous uncertainties are involved in the microgrid operation scheduling problems for both short-term and longer term. Those uncertainties may result in a non-optimal operation or even jeopardizing the reliability of the microgrid operation if they are not fully considered.

In this dissertation, the uncertainties in the microgrid operation are addressed by stochastic modeling and optimization techniques. The microgrid day-ahead scheduling problem, demand side management scheduling problem, and medium-term operation scheduling problem are modelled via stochastic approaches to achieve the optimal operation decisions under a stochastic environment. Meanwhile, a microgrid carbon emission co-optimized scheduling problem is also proposed to address the carbon emission in the microgrid operation. Correspondingly, the uncertainty models and solving methods for those formulations are also proposed and numerical results are presented for verification and illustration purpose.

Considering the development of smart grid technologies, the microgrid can act as a role model from the bulk power system point of view. There are still rooms for improvement between the interaction of microgrid and bulk power system in the current deregulated power market. In this dissertation, the procurement portfolio optimization for

microgrid has been discussed while treating the day-ahead market and real-time market as stochastic price scenarios. A future study regarding the microgrid operation can be the optimal offering and bidding strategy to participate in the wholesale power market.

Moreover, considering the characteristics of stochastic optimization techniques, a dynamic security constrained operation scheduling problem for microgrid can be further explored. For a microgrid which has their value of lost load as a time-variant function, this formulation and dynamic load shedding scheme can be effective approaches to improve the operation efficiency of the microgrid.

Furthermore, the uncertainty modeling techniques for different type of microgrid require further investigation. The estimation of the probability distribution of the renewable generation for different scales, the price responsive patterns of end users from different load classes and the value of lost load for different operation periods play critical roles in the optimal operation of microgrid. It will benefit the microgrid operation significantly if those forecasting and estimation accuracy can be improved based on the current development of smart meter installation and big data techniques.

Appendix A

Nomenclature for Chapter 3, Chapter 4 and Chapter 5

Indices and Sets

I	Set of all fossil-fuel generators, index by i
S	Set of all scenarios of random parameters, index by s
T	Set of all operation period, index by t

System Parameters and Functions

p_t^{Wind}	Aggregated wind generation output in t
p_t^{Pv}	Aggregated solar generation output in t
p_t^{Load}	Aggregated microgrid total demand in t
$p_{t,s}^{Wind}$	Aggregated wind generation output in t for scenario s
$p_{t,s}^{Pv}$	Aggregated solar generation output in t for scenario s
$p_{t,s}^{Load}$	Aggregated microgrid load in t for scenario s
$P_{i,\min}$	Minimum power output of fossil-fuel generator i
$P_{i,\max}$	Maximum power output of fossil-fuel generator i
$P_{\max}^{Char}$	Maximum charging power of energy storage system
$P_{\max}^{Dischar}$	Maximum discharging power of energy storage system
$E_{\min}^{Stor}$	Minimum storage level of energy storage system
$E_{\max}^{Stor}$	Maximum storage level of energy storage system
E_t^{Stor}	Storage level of energy storage system at the end operation period t
E_{ini}^{Stor}	Initial storage level of energy storage system at the beginning of the operation horizon
E_{final}^{Stor}	Final storage level of energy storage system at the end of the operation horizon
$\eta_{Dischar}$	Discharge efficiency of energy storage system
η_{Char}	Charge efficiency of energy storage system
λ_t	Penalty cost for unserved load in t
V_t	Amount of unserved load in t
$V_{t,s}$	Amount of unserved load in t for scenario s
RD_i	Ramp-down rate for fossil-fuel generator i
RU_i	Ramp-up rate for fossil-fuel generator i
MU_i	Minimum-up time for fossil-fuel generator i
MD_i	Minimum-down time for fossil-fuel generator i
SU_i	Start-up cost for fossil-fuel generator i
SD_i	Shut-down cost for fossil-fuel generator i
O_i	No load cost for fossil-fuel generator i
C_i	Marginal cost of fossil-fuel generator i in t
R_t	Microgrid operation reserve requirement
SU_i^E	Start-up carbon emission for fossil-fuel generator i
SD_i^E	Shut-down carbon emission for fossil-fuel generator i
O_i^E	No load carbon emission for fossil-fuel generator i

C_i^E	Marginal carbon emission of fossil-fuel generator *i* in *t*
π	Carbon emission price
r	Probability of scheduled generations do not meet microgrid demand (operation risk)
N	Total number of scenarios in set *S*
	Decision variables
$p_{i,t}$	Power output of fossil-fuel generator *i* in *t*
$p_t^{DisChar}$	Discharging power of energy storage system in *t*
p_t^{Char}	Charging power of energy storage system in *t*
$o_{i,t}$	Binary variable to indicate if fossil-fuel generator *i* is on in *t*
$u_{i,t}$	Binary variable to indicate if fossil-fuel generator *i* is started up in *t*
$v_{i,t}$	Binary variable to indicate if fossil-fuel generator *i* is shut down in *t*
x_t	Binary variable to indicate if probabilistic constraint is satisfied in *t*
y_t	Binary variable to indicate if there is positive amount of unserved load in *t*
z_t	Binary variable to indicate if energy storage is discharging in *t*
$\Delta\pi_t$	Price change from the base price in t

.

Appendix B

Nomenclature for Chapter 6

Indices and Sets

I	Set of all load classes, index by i
S	Set of all realizations of random vector, index by s
T	Set of all operation periods, index by t
T_{PWD}	Set of peak weekday operation periods, index by t
T_{PWE}	Set of peak weekend operation periods, index by t
T_{OP}	Set of off peak operation periods, index by t

Parameters

π^F_{PWD}	Price of peak weekday forward contract
π^F_{PWE}	Price of peak weekend forward contract
π^F_{OP}	Price of off peak forward contract
$E^F_{PWD,\max}$	Upper energy volume bound for peak weekday forward contract
$E^F_{PWD,\min}$	Lower energy volume bound for peak weekday forward contract
$E^F_{PWE,\max}$	Upper energy volume bound for peak weekend forward contract
$E^F_{PWE,\min}$	Lower energy volume bound for peak weekend forward contract
$E^F_{OP,\max}$	Upper energy volume bound for off peak forward contract
$E^F_{OP,\min}$	Lower energy volume bound for off peak forward contract
$p^F_{PWD,\max}$	Upper bound of energy consumption in operation period for peak weekday forward contract
$p^F_{PWD,\min}$	Lower bound of energy consumption in operation period for peak weekday forward contract
$p^F_{PWE,\max}$	Upper bound of energy consumption in operation period for peak weekend forward contract
$p^F_{PWE,\min}$	Lower bound of energy consumption in operation period for peak weekend forward contract
$p^F_{OP,\max}$	Upper bound of energy consumption in operation period for off peak forward contract
$p^F_{OP,\min}$	Lower bound of energy consumption in operation period for off peak forward contract
$prob_s$	Probability of scenario s
$\pi^{DA}_{t,s}$	Settlement price of day-ahead market at t for scenario s
$\pi^{DA}_{t,s}$	Settlement price of real-time market at t for scenario s
β	Risk coefficient
$p^{Loadi}_{t,s}$	Demand for load class i at t for scenario s after demand side management
$p^{Loadi}_{t,base}$	Base demand for load class i at t before demand side management
ε^{Loadi}_t	Price elasticity for load class i at t
$\pi^{Eff}_{t,s}$	Effective price for the demand side management at t for scenario s

Decision variables

p_{PWD}^{F}	Energy procurement from peak weekday forward contract
p_{PWE}^{F}	Energy procurement from peak weekend forward contract
p_{OP}^{F}	Energy procurement from off peak forward contract
$p_{t,s}^{DA}$	Energy procurement settled in day-ahead market at *t* for scenario *s*
$p_{t,s}^{RT}$	Energy procurement settled in real-time market at *t* for scenario *s*

References

[1] R. H. Lasseter, "MicroGrids," in *Power Engineering Society Winter Meeting, 2002. IEEE*, 2002, pp. 305-308 vol.1.

[2] R. Lasseter, A. Akhil, C. Marnay, J. Stephens, J. Dagle, R. Guttromson, A. S. Meliopoulous, R. Yinger, and J. Eto, "Integration of distributed energy resources. The CERTS Microgrid Concept," ed, 2002.

[3] S. Bossart, "DOE Perspective on Microgrids," in *Advanced Microgrid Concepts and Technologies Workshop*, 2012.

[4] S. Van Broekhoven, N. Judson, S. Nguyen, and W. Ross, "Microgrid Study: Energy Security for DoD Installations," DTIC Document2012.

[5] W.-J. Lee and D. Wetz, "Development of a Smart MicroGrid Testbed," 2013.

[6] N. Hatziargyriou, H. Asano, R. Iranvani, and C. Marnay, "Microgrids: An Overview of Ongoing Research, Development, and Demonstration Projects," Ernest Orlando Lawrence Berkeley National LaboratoryJuly 2007.

[7] M. Barnes, A. Dimeas, A. Engler, C. Fitzer, N. Hatziargyriou, C. Jones, S. Papathanassiou, and M. Vandenbergh, "Microgrid laboratory facilities," in *Future Power Systems, 2005 International Conference on*, 2005, pp. 6 pp.-6.

[8] S. Morozumi, "Micro-grid Demonstration Projects in Japan," in *Power Conversion Conference - Nagoya, 2007. PCC '07*, 2007, pp. 635-642.

[9] M. Barnes, J. Kondoh, H. Asano, J. Oyarzabal, G. Ventakaramanan, R. Lasseter, N. Hatziargyriou, and T. Green, "Real-World MicroGrids-An Overview," in *System of Systems Engineering, 2007. SoSE '07. IEEE International Conference on*, 2007, pp. 1-8.

[10] M. Shahidehpour, M. Khodayar, and M. Barati, "Campus microgrid: High reliability for active distribution systems," in *Power and Energy Society General Meeting, 2012 IEEE*, 2012, pp. 1-2.

[11] National Instruments. (2012). *National Instruments CompactRIO*. Available: http://www.ni.com/compactrio/

[12] M. LeMay, R. Nelli, G. Gross, and C. A. Gunter, "An integrated architecture for demand response communications and control," in *Hawaii International Conference on System Sciences, Proceedings of the 41st Annual*, 2008, pp. 174-174.

[13] P. Fuangfoo, T. Meenual, W.-j. Lee, and C. C. Inwai, "PEA Guidelines of Impact Study and Operation of DG for Islanding Operation," in *Industrial & Commercial Power Systems Technical Conference, 2007. ICPS 2007. IEEE/IAS*, 2007, pp. 1-5.

[14] World Bank. (2014). *Energy Facts*. Available: http://www.worldbank.org/en/topic/energy

[15] Z. Ding, W.-J. Lee, D. Wetz, and C.-C. Tsai, "Evaluating the use of a MicroGrid as a Power Solution for Africa's Rural Areas," in *Power & Energy Sociey General Meeting, 2009. PES'12. IEEE*, San Deigo, CA, 2012, pp. 1-5.

[16] Z. Ding, M. Liu, W.-J. Lee, and D. Wetz, "An autonomous operation microgrid for rural electrification," in *Industry Applications Society Annual Meeting, 2013 IEEE*, 2013, pp. 1-8.

[17] Z. Ding, W.-J. Lee, and J. Wang, "Stochastic Resource Planning Strategy to Improve the Efficiency of Microgrid Operation," *Industry Applications, IEEE Transactions on,* vol. PP, pp. 1-1, 2014.

[18] S. Lu, Y. V. Makarov, C. A. McKinstry, A. J. Brothers, and S. Jin, "Low Probability Tail Event Analysis and Mitigation in the BPA Control Area: Task 2 Report," Pacific Northwest National Laboratory (PNNL), Richland, WA (US)2009.

[19] ERCOT, "ERCOT Monthly Operational Overview," ed, 2013.

[20] N. Lu, R. Diao, R. P. Hafen, N. Samaan, and Y. V. Makarov, "A comparison of forecast error generators for modeling wind and load uncertainty," in *Power and Energy Society General Meeting (PES), 2013 IEEE*, 2013, pp. 1-5.

[21] P. ECONOMICS, "2012 State of the Market Report for the ERCOT Wholesale Electricity Markets," POTOMAC ECONOMICS2013.

[22] Y. V. Makarov, Z. Huang, P. V. Etingov, J. Ma, R. T. Guttromson, K. Subbarao, and B. B. Chakrabarti, "Wind Energy Management System EMS Integration Project: Incorporating Wind Generation and Load Forecast Uncertainties into Power Grid Operations," Pacific Northwest National Laboratory (PNNL), Richland, WA (US)2010.

[23] B. Hodge, A. Florita, K. Orwig, D. Lew, and M. Milligan, "Comparison of Wind Power and Load Forecasting Error Distributions: Preprint," National Renewable Energy Laboratory (NREL), Golden, CO.2012.

[24] E. Ela, V. Diakov, E. Ibanez, and M. Heaney, "Impacts of Variability and Uncertainty in Solar Photovoltaic Generation at Multiple Timescales," National Renewable Energy Laboratory (NREL), Golden, CO.2013.

[25] R. Barth, P. Meibom, and C. Weber, "Simulation of short-term forecasts of wind and load for a stochastic scheduling model," in *Power and Energy Society General Meeting, 2011 IEEE*, 2011, pp. 1-8.

[26] K. Methaprayoon, C. Yingvivatanapong, W.-j. Lee, and J. R. Liao, "An Integration of ANN Wind Power Estimation Into Unit Commitment Considering the Forecasting

Uncertainty," *Industry Applications, IEEE Transactions on,* vol. 43, pp. 1441-1448, 2007.

[27] B. M. Hodge, D. Lew, and M. Milligan, "Short-Term Load Forecast Error Distributions and Implications for Renewable Integration Studies," in *Green Technologies Conference, 2013 IEEE*, 2013, pp. 435-442.

[28] S. Fan, J. R. Liao, R. Yokoyama, L. Chen, and W.-J. Lee, "Forecasting the Wind Generation Using a Two-Stage Network Based on Meteorological Information," *Energy Conversion, IEEE Transactions on,* vol. 24, pp. 474-482, 2009.

[29] B. Neenan and J. Eom, "Price elasticity of demand for electricity: a primer and synthesis," *Electric Power Research Institute,* 2008.

[30] P. R. Thimmapuram and K. Jinho, "Consumers' Price Elasticity of Demand Modeling With Economic Effects on Electricity Markets Using an Agent-Based Model," *Smart Grid, IEEE Transactions on,* vol. 4, pp. 390-397, 2013.

[31] D. Ton, M. A. Biviji, E. Nagypal, and J. Wang, "Tool for determining price elasticity of electricity demand and designing dynamic price program," in *Innovative Smart Grid Technologies (ISGT), 2013 IEEE PES*, 2013, pp. 1-6.

[32] P. Thorsnes, J. Williams, and R. Lawson, "Consumer responses to time varying prices for electricity," *Energy Policy,* vol. 49, pp. 552-561, 2012.

[33] S. Fan and R. J. Hyndman, "The price elasticity of electricity demand in South Australia," *Energy Policy,* vol. 39, pp. 3709-3719, 2011.

[34] A. Shapiro and A. P. Ruszczyński, *Stochastic programming*: Elsevier, 2003.

[35] C. A. Hernandez-Aramburo, T. C. Green, and N. Mugniot, "Fuel consumption minimization of a microgrid," *Industry Applications, IEEE Transactions on,* vol. 41, pp. 673-681, 2005.

[36] W. Su, Z. Yuan, and M.-Y. Chow, "Microgrid planning and operation: Solar energy and wind energy," in *Power and Energy Society General Meeting, 2010 IEEE*, 2010, pp. 1-7.

[37] C. Chen, S. Duan, T. Cai, B. Liu, and G. Hu, "Smart energy management system for optimal microgrid economic operation," *Renewable Power Generation, IET,* vol. 5, pp. 258-267, 2011.

[38] A. Khodaei and M. Shahidehpour, "Optimal operation of a community-based microgrid," in *Innovative Smart Grid Technologies Asia (ISGT), 2011 IEEE PES*, 2011, pp. 1-3.

[39] A. Milo, H. Gaztanaga, I. Etxeberria-Otadui, E. Bilbao, and P. Rodriguez, "Optimization of an experimental hybrid microgrid operation: Reliability and economic issues," in *PowerTech, 2009 IEEE Bucharest*, 2009, pp. 1-6.

[40] A. K. Basu, A. Bhattacharya, S. Chowdhury, and S. P. Chowdhury, "Planned Scheduling for Economic Power Sharing in a CHP-Based Micro-Grid," *Power Systems, IEEE Transactions on,* vol. 27, pp. 30-38, 2012.

[41] S. Conti, R. Nicolosi, S. A. Rizzo, and H. H. Zeineldin, "Optimal Dispatching of Distributed Generators and Storage Systems for MV Islanded Microgrids," *Power Delivery, IEEE Transactions on,* vol. 27, pp. 1243-1251, 2012.

[42] P. Meibom, R. Barth, B. Hasche, H. Brand, C. Weber, and M. O"Malley, "Stochastic Optimization Model to Study the Operational Impacts of High Wind Penetrations in Ireland," *Power Systems, IEEE Transactions on,* vol. 26, pp. 1367-1379, 2011.

[43] V. S. Pappala, I. Erlich, K. Rohrig, and J. Dobschinski, "A Stochastic Model for the Optimal Operation of a Wind-Thermal Power System," *Power Systems, IEEE Transactions on,* vol. 24, pp. 940-950, 2009.

[44] A. Y. Saber and G. K. Venayagamoorthy, "Resource scheduling under uncertainty in a smart grid with renewables and plug-in vehicles," *Systems Journal, IEEE,* vol. 6, pp. 103-109, 2012.

[45] J. J. Hargreaves and B. F. Hobbs, "Commitment and Dispatch With Uncertain Wind Generation by Dynamic Programming," *Sustainable Energy, IEEE Transactions on,* vol. 3, pp. 724-734, 2012.

[46] K. K. Kariuki and R. N. Allan, "Evaluation of reliability worth and value of lost load," *Generation, Transmission and Distribution, IEE Proceedings-,* vol. 143, pp. 171-180, 1996.

[47] D. S. Kirschen, K. R. W. Bell, D. P. Nedic, D. Jayaweera, and R. N. Allan, "Computing the value of security," *Generation, Transmission and Distribution, IEE Proceedings,* vol. 150, pp. 673-678, 2003.

[48] J. Hu, T. Homem-de-Mello, and S. Mehrotra, "Sample average approximation of stochastic dominance constrained programs," *Mathematical programming,* vol. 133, pp. 171-201, 2012.

[49] Z. Shu and P. Jirutitijaroen, "Latin hypercube sampling techniques for power systems reliability analysis with renewable energy sources," *Power Systems, IEEE Transactions on,* vol. 26, pp. 2066-2073, 2011.

[50] S. Ahmed and A. Shapiro, "Solving chance-constrained stochastic programs via sampling and integer programming," *Tutorials in Operations Research,(Z.-L. Chen and S. Raghavan, eds.), INFORMS,* vol. 2008, 2008.

[51] J. Luedtke, S. Ahmed, and G. L. Nemhauser, "An integer programming approach for linear programs with probabilistic constraints," *Mathematical programming,* vol. 122, pp. 247-272, 2010.

[52] A. J. Miller and L. A. Wolsey, "Tight formulations for some simple mixed integer programs and convex objective integer programs," *Mathematical programming,* vol. 98, pp. 73-88, 2003.

[53] IBM . CPLEX. (2013). *V12. 5: Users manual for CPLEX*. Available: http://pic.dhe.ibm.com/infocenter/cosinfoc/v12r5/index.jsp

[54] London Economics, "Estimating the Value of Lost Load," ERCOT, ERCOT 2013.

[55] U. Parliament, "Climate change act 2008," *London, UK,* 2008.

[56] F. J. Convery and L. Redmond, "Market and price developments in the European Union emissions trading scheme," *Review of Environmental Economics and Policy,* vol. 1, pp. 88-111, 2007.

[57] C. F. t. Commission, "Europe 2020: a strategy for smart, sustainable and inclusive growth," *Brussels: European Commission,* 2010.

[58] *Clean Power Plan Proposed Rule*. Available: http://www2.epa.gov/carbon-pollution-standards/clean-power-plan-proposed-rule

[59] M. Muslu, "Economic dispatch with environmental considerations: tradeoff curves and emission reduction rates," *Electric Power Systems Research,* vol. 71, pp. 153-158, 2004.

[60] Z. Ji, C. Kang, Q. Chen, Q. Xia, C. Jiang, Z. Chen, and J. Xin, "Low-Carbon Power System Dispatch Incorporating Carbon Capture Power Plants," *Power Systems, IEEE Transactions on,* vol. 28, pp. 4615-4623, 2013.

[61] M. Reza Norouzi, A. Ahmadi, A. Esmaeel Nezhad, and A. Ghaedi, "Mixed integer programming of multi-objective security-constrained hydro/thermal unit commitment," *Renewable and Sustainable Energy Reviews,* vol. 29, pp. 911-923, 2014.

[62] M. A. Abido, "Multiobjective particle swarm optimization for environmental/economic dispatch problem," *Electric Power Systems Research,* vol. 79, pp. 1105-1113, 2009.

[63] C. Wang, Z. Lu, and Y. Qiao, "A Consideration of the Wind Power Benefits in Day-Ahead Scheduling of Wind-Coal Intensive Power Systems," *Power Systems, IEEE Transactions on,* vol. 28, pp. 236-245, 2013.

[64] Y. Lu, J. Zhou, H. Qin, Y. Wang, and Y. Zhang, "A hybrid multi-objective cultural algorithm for short-term environmental/economic hydrothermal scheduling," *Energy Conversion and Management,* vol. 52, pp. 2121-2134, 2011.

[65] L. Xie and M. D. Ilic, "Emission-concerned economic dispatch: Possible formulations and implementations," in *Transmission and Distribution Conference and Exposition, 2010 IEEE PES*, 2010, pp. 1-6.

[66] C. Kang, X. Chen, Q. Xu, D. Ren, Y. Huang, Q. Xia, W. Wang, C. Jiang, J. Liang, J. Xin, X. Chen, B. Peng, K. Men, Z. Chen, X. Jin, H. Li, and J. Huang, "Balance of Power: Toward a More Environmentally Friendly, Efficient, and Effective Integration of Energy Systems in China," *Power and Energy Magazine, IEEE,* vol. 11, pp. 56-64, 2013.

[67] S. Succar and R. H. Williams, "Compressed air energy storage: Theory, resources, and applications for wind power," *Princeton environmental institute report,* vol. 8, 2008.

[68] M. H. Albadi and E. F. El-Saadany, "Demand Response in Electricity Markets: An Overview," in *Power Engineering Society General Meeting, 2007. IEEE*, 2007, pp. 1-5.

[69] N. Mankiw, *Principles of microeconomics*: Cengage Learning, 2014.

[70] Y. Simmhan, S. Aman, A. Kumbhare, R. Liu, S. Stevens, Q. Zhou, and V. Prasanna, "Cloud-Based Software Platform for Big Data Analytics in Smart Grids," *Computing in Science & Engineering,* vol. 15, pp. 38-47, 2013.

[71] R. Palma-Behnke, C. Benavides, F. Lanas, B. Severino, L. Reyes, J. Llanos, and D. Saez, "A Microgrid Energy Management System Based on the Rolling Horizon Strategy," *Smart Grid, IEEE Transactions on,* vol. 4, pp. 996-1006, 2013.

[72] C. O. Adika and W. Lingfeng, "Autonomous Appliance Scheduling for Household Energy Management," *Smart Grid, IEEE Transactions on,* vol. 5, pp. 673-682, 2014.

[73] C. Gouveia, J. Moreira, C. L. Moreira, and J. A. Pecas Lopes, "Coordinating Storage and Demand Response for Microgrid Emergency Operation," *Smart Grid, IEEE Transactions on,* vol. 4, pp. 1898-1908, 2013.

[74] S. A. Pourmousavi and M. H. Nehrir, "Real-Time Central Demand Response for Primary Frequency Regulation in Microgrids," *Smart Grid, IEEE Transactions on,* vol. 3, pp. 1988-1996, 2012.

[75] D. Wang, S. Ge, H. Jia, C. Wang, Y. Zhou, N. Lu, and X. Kong, "A Demand Response and Battery Storage Coordination Algorithm for Providing Microgrid Tie-Line Smoothing Services," *Sustainable Energy, IEEE Transactions on,* vol. 5, pp. 476-486, 2014.

[76] M. Tasdighi, H. Ghasemi, and A. Rahimi-Kian, "Residential Microgrid Scheduling Based on Smart Meters Data and Temperature Dependent Thermal Load Modeling," *Smart Grid, IEEE Transactions on,* vol. 5, pp. 349-357, 2014.

[77] F. Farzan, S. Lahiri, M. Kleinberg, K. Gharieh, and M. Jafari, "Microgrids for Fun and Profit: The Economics of Installation Investments and Operations," *Power and Energy Magazine, IEEE,* vol. 11, pp. 52-58, 2013.

[78] M. Shahidehpour and M. Khodayar, "Cutting Campus Energy Costs with Hierarchical Control: The Economical and Reliable Operation of a Microgrid," *Electrification Magazine, IEEE,* vol. 1, pp. 40-56, 2013.

[79] EPRI, "Price Elasticiy of Demand for Electricity: A Primer and Synthesis," EPRI 2008.

[80] D. S. Kirschen, G. Strbac, P. Cumperayot, and D. de Paiva Mendes, "Factoring the elasticity of demand in electricity prices," *Power Systems, IEEE Transactions on,* vol. 15, pp. 612-617, 2000.

[81] A. Faruqui and R. Hledik, "California's next generation of load management standards," California Energy Commission2007.

[82] S. Borenstein, "Effective and Equitable Adoption of Opt-In Residential Dynamic Electricity Pricing," *Review of Industrial Organization,* vol. 42, pp. 127-160, 2013/03/01 2013.

[83] Navigant, "Net Metering Bill Impacts and Distributed Energy Subsidies," Arizona Public Service2012.

[84] A. Tuohy, P. Meibom, E. Denny, and M. O'Malley, "Benefits of Stochastic Scheduling for Power Systems with Significant Installed Wind Power," in *Probabilistic Methods Applied to Power Systems, 2008. PMAPS '08. Proceedings of the 10th International Conference on*, 2008, pp. 1-7.

[85] K. M. Anstreicher, "On convex relaxations for quadratically constrained quadratic programming," *Mathematical programming,* vol. 136, pp. 233-251, 2012.

[86] N. Y. Soltani, S.-J. Kim, and G. B. Giannakis, "Online learning of load elasticity for electric vehicle charging," in *Computational Advances in Multi-Sensor Adaptive Processing (CAMSAP), 2013 IEEE 5th International Workshop on*, 2013, pp. 436-439.

[87] J. Yu, S. Teng, and J. Mickey, "Evolution of ERCOT Market," in *Transmission and Distribution Conference and Exhibition: Asia and Pacific, 2005 IEEE/PES*, 2005, pp. 1-6.

[88] D. Chen, "Post-market computation engine toward CAISO market settlements," in *Transmission and Distribution Conference and Exposition, 2008. T&D. IEEE/PES*, 2008, pp. 1-8.

[89] P. Mandal, T. Senjyu, N. Urasaki, T. Funabashi, and A. K. Srivastava, "Electricity Price Forecasting for PJM Day-Ahead Market," in *Power Systems Conference and Exposition, 2006. PSCE '06. 2006 IEEE PES*, 2006, pp. 1321-1326.

[90] R. Jones, "Midwest ISO experience with reliability unit commitment," in *Power Engineering Society General Meeting, 2006. IEEE*, 2006, p. 1 pp.

[91] K. B. Sahay and M. M. Tripathi, "Day ahead hourly load forecast of PJM electricity market and ISO New England market by using artificial neural network," in *Innovative Smart Grid Technologies - Asia (ISGT Asia), 2013 IEEE*, 2013, pp. 1-5.

[92] N. Zhang, T. Mount, and R. Boisvert, "Generators Bidding Behavior in the NYISO Day-Ahead Wholesale Electricity Market," in *System Sciences, 2007. HICSS 2007. 40th Annual Hawaii International Conference on*, 2007, pp. 123-123.

[93] M. Shahidehpour, H. Yamin, and Z. Li, *Market Operations in Electric Power Systems*: John Wiley & Sons, Inc., 2002.

[94] Y. a. Liu and X. Guan, "Purchase allocation and demand bidding in electric power markets," *Power Systems, IEEE Transactions on,* vol. 18, pp. 106-112, 2003.

[95] C.-K. Woo, R. I. Karimov, and I. Horowitz, "Managing electricity procurement cost and risk by a local distribution company," *Energy Policy,* vol. 32, pp. 635-645, 2004.

[96] J. Xu, P. B. Luh, F. B. White, E. Ni, and K. Kasiviswanathan, "Power Portfolio Optimization in Deregulated Electricity Markets With Risk Management," *Power Systems, IEEE Transactions on,* vol. 21, pp. 1653-1662, 2006.

[97] J. Kettunen, A. Salo, and D. W. Bunn, "Optimization of Electricity Retailer's Contract Portfolio Subject to Risk Preferences," *Power Systems, IEEE Transactions on,* vol. 25, pp. 117-128, 2010.

[98] C.-K. Woo, I. Horowitz, B. Horii, and R. I. Karimov, "The efficient frontier for spot and forward purchases: an application to electricity," *Journal of the Operational Research Society,* vol. 55, pp. 1130-1136, 2004.

[99] M. Carrion, A. J. Conejo, and J. M. Arroyo, "Forward Contracting and Selling Price Determination for a Retailer," *Power Systems, IEEE Transactions on,* vol. 22, pp. 2105-2114, 2007.

[100] M. Carrion, J. M. Arroyo, and A. J. Conejo, "A Bilevel Stochastic Programming Approach for Retailer Futures Market Trading," *Power Systems, IEEE Transactions on,* vol. 24, pp. 1446-1456, 2009.

[101] *ERCOT Nodal Protocols*. Available: http://www.ercot.com/mktrules/nprotocols/

[102] S. Mohagheghi and N. Raji, "Dynamic demand response solution for industrial customers," in *Industry Applications Society Annual Meeting, 2013 IEEE*, 2013, pp. 1-9.

[103] S. Mohagheghi and N. Raji, "Intelligent demand response scheme for energy management of industrial systems," in *Industry Applications Society Annual Meeting (IAS), 2012 IEEE*, 2012, pp. 1-9.

[104] L. Zhang, J. Zhao, X. Han, and L. Niu, "Day-ahead Generation Scheduling with Demand Response," in *Transmission and Distribution Conference and Exhibition: Asia and Pacific, 2005 IEEE/PES*, 2005, pp. 1-4.

[105] D. Li and W. L. Ng, "Optimal Dynamic Portfolio Selection: Multiperiod Mean-Variance Formulation," *Mathematical Finance,* vol. 10, pp. 387-406, 2000.

[106] H. M. Markowitz, "Foundations of portfolio theory," *The journal of finance,* vol. 46, pp. 469-477, 1991.

[107] P. Wang, H. Zareipour, and W. D. Rosehart, "Descriptive Models for Reserve and Regulation Prices in Competitive Electricity Markets," *Smart Grid, IEEE Transactions on,* vol. 5, pp. 471-479, 2014.

[108] K. Zare, M. P. Moghaddam, and M. K. Sheikh-El-Eslami, "Risk-Based Electricity Procurement for Large Consumers," *Power Systems, IEEE Transactions on,* vol. 26, pp. 1826-1835, 2011.

[109] P. Bajpai and S. N. Singh, "Fuzzy Adaptive Particle Swarm Optimization for Bidding Strategy in Uniform Price Spot Market," *Power Systems, IEEE Transactions on,* vol. 22, pp. 2152-2160, 2007.

[110] J. Janczura and R. Weron, "Regime-switching models for electricity spot prices: Introducing heteroskedastic base regime dynamics and shifted spike distributions," in *Energy Market, 2009. EEM 2009. 6th International Conference on the European*, 2009, pp. 1-6.

[111] ERCOT. Load Zone Price Data [Online]. Available: http://mis.ercot.com/misapp/GetReports.do?reportTypeId=12300&reportTitle=LMPs%20by%20Resource%20Nodes,%20Load%20Zones%20and%20Trading%20Hubs&showHTMLView=&mimicKey

[112] W. D. Kelton, R. P. Sadowski, and D. A. Sadowski, *Simulation with ARENA* vol. 3: McGraw-Hill New York, 2002.

[113] C. A. Holt and S. K. Laury, "Risk aversion and incentive effects," *American economic review,* vol. 92, pp. 1644-1655, 2002.

[114] M. Rabin, "Risk aversion and expected-utility theory: A calibration theorem," *Econometrica,* vol. 68, pp. 1281-1292, 2000.

[115] L. P. Hansen and K. J. Singleton, "Stochastic consumption, risk aversion, and the temporal behavior of asset returns," *The Journal of Political Economy,* pp. 249-265, 1983.

[116] P. Weil, "The equity premium puzzle and the risk-free rate puzzle," *Journal of Monetary Economics,* vol. 24, pp. 401-421, 1989.

Biographical Information

Zhaohao Ding was born in Binzhou, Shandong, China, in 1988. He received both his B.S. in Electrical Engineering and B.A. in Finance from Shandong University, Jinan, China in June 2010. In August 2010, he joined Energy Systems Research Center (ESRC) with Provost-level Scholarship at the University of Texas at Arlington to pursue his Ph.D. degree in the area of power system operation optimization. His research areas of interest include power system operation and planning, power market, and stochastic optimization applications in power system.